ACS Chemical Biology. 13 (5): 1260-1269 (2018).

Identification and Characterization of Small Molecule Compounds That Modulate Trichothecene Production by *Fusarium graminearum*

Kazuyuki Maeda[†,‡], Hinayo Ichikawa[†], Yuichi Nakajima[†], Takayuki Motoyama[§], Shuichi Ohsato[‡], Kyoko Kanamaru[†], Tetsuo Kobayashi[†], Takumi Nishiuchi[∥], Hiroyuki Osada[§], Makoto Kimura[*,†]

[†] Graduate School of Bioagricultural Sciences, Nagoya University, Furo-cho, Chikusa-ku, Nagoya, Aichi 464-8601, Japan

[‡] Graduate School of Agriculture, Meiji University, 1-1-1 Higashi-Mita, Kawasaki, Kanagawa 214-8571, Japan

[§] Chemical Biology Research Group, RIKEN Center for Sustainable Resource Science, 2-1 Hirosawa, Wako, Saitama 351-0198, Japan

[∥] Advanced Science Research Centre, Kanazawa University, 13-1 Takaramachi, Kanazawa, Ishikawa 920-0934, Japan

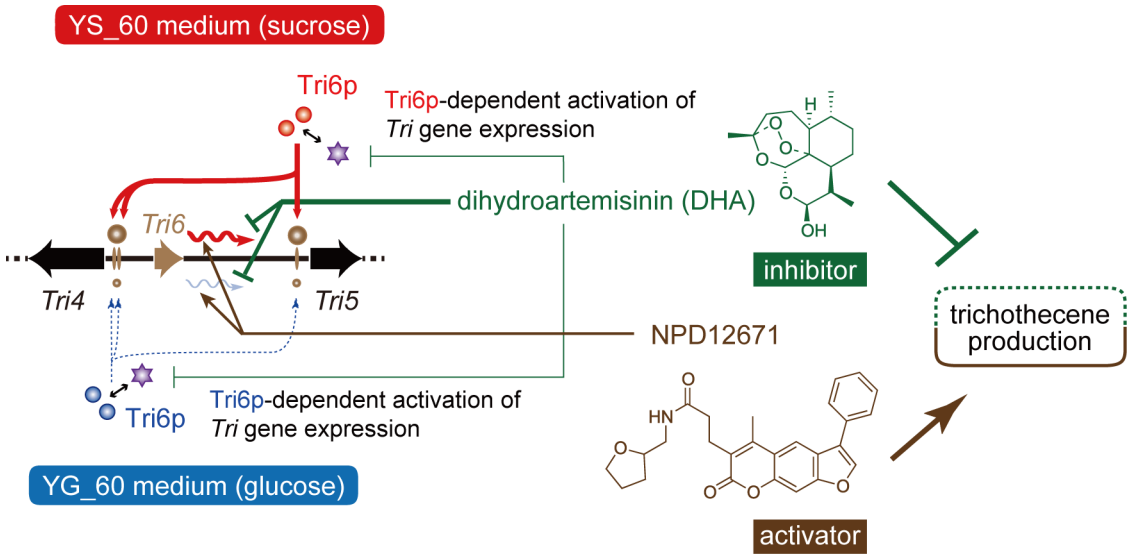
YS_60 medium (sucrose)
Tri6p
Tri6p-dependent activation of
Tri gene expression
dihydroartemisinin (DHA)
Tri6
Tri4
Tri5
inhibitor
trichothecene
production
NPD12671
Tri6p
Tri6p-dependent activation of
Tri gene expression
YG_60 medium (glucose)
activator

ABSTRACT

From the RIKEN Natural Products Depository (NPDepo) chemical library, we identified small molecules that alter trichothecene 15-acetyldeoxynivalenol (15-ADON) production by *Fusarium graminearum*. Among trichothecene production activators, a furanocoumarin NPD12671 showed the strongest stimulatory activity on 15-ADON production by the fungus cultured in a 24-well plate. NPD12671 significantly increased the transcription of *Tri6*, a transcription factor gene necessary for trichothecene biosynthesis, in both trichothecene-inducing and non-inducing culture conditions. Dihydroartemisinin (DHA) was identified as the most effective inhibitor of trichothecene production in 24-well plate culture; DHA inhibited trichothecene production (>50% inhibition at 1 μM) without affecting fungal mass by suppressing *Tri6* expression. To determine the effect of DHA on trichothecene pathway *Tri* gene expression, we generated a constitutively *Tri6*-overexpressing strain that produced 15-ADON in YG_60 medium in Erlenmeyer flasks, conditions under which no trichothecenes are produced by the wild-type. While 5 μM DHA failed to inhibit trichothecene biosynthesis by the overexpressor in trichothecene-inducing YS_60 culture, trichothecene production was suppressed in the YG_60 culture. Regardless of a high *Tri6* transcript level in the constitutive overexpressor, the YG_60 culture showed reduced accumulation of *Tri5* and *Tri4* mRNA upon treatment with 5 μM DHA. Deletion mutants of *FgOs2* were also generated and examined; both NPD12671 and DHA modulated trichothecene production as they did in the wild-type strain. These results are discussed in light of the mode of actions of these chemicals on trichothecene biosynthesis.

Cereal grains are often contaminated with a group of mycotoxin known as trichothecenes. These sesquiterpenoid mycotoxins, characterized by the presence of a 9,10-double bond and a 12,13-epoxide, are produced by several plant pathogenic *Fusarium* species.[1, 2] Above all, the *Fusarium graminearum* species complex is an important group of fungi that causes ear rot in maize and head blight in wheat and barley. These pathogens contaminate infected grains with trichothecene mycotoxins, such as deoxynivalenol (DON), 3-acetyldeoxynivalenol (3-ADON), 15-acetyldeoxynivalenol (15-ADON), and nivalenol (NIV). These mycotoxins are potent inhibitors of eukaryotic protein synthesis and cause acute adverse health effects in humans and animals.[3]

Most genes involved in trichothecene biosynthesis (*Tri* genes) were found in a cluster and their functions have been elucidated.[4-6] Among the *Tri* genes, only *Tri5*, *Tri4*, *Tri6*, and *Tri10* are necessary to synthesize a trichothecene skeleton.[1, 2] *Tri5* and *Tri4* encode a trichodiene synthase[7] and multifunctional trichodiene monooxygenase,[8, 9] respectively, and provide the first trichothecene isotrichodermol from farnesyl pyrophosphate (FPP).[1, 10] *Tri6* encodes a Cys_2His_2 zinc finger transcription factor[11] that is indispensable for transcription of pathway *Tri* genes. Tri6p also positively regulates transcription of genes encoding proteins involved in isoprenoid biosynthesis and increases FPP levels.[12] In addition, transcription of *Tri* genes is critically dependent on a biochemically uncharacterized regulatory protein encoded by *Tri10*.[13] Although the essentiality of *Tri6* and *Tri10* for trichothecene biosynthesis was demonstrated in previous studies,[11, 13] molecular mechanisms underlying transcriptional control of these regulatory genes, as well as their protein interactions and functional roles in transcription of other *Tri* genes, remain to be clarified.

Certain nutritional and environmental conditions regulate trichothecene production in axenic *F. graminearum* cultures. Carbon sources and media pH are important factors for fungal secondary metabolism, and this holds true for *F.*

graminearum.[14, 15] The quality and quantity of nitrogen are also important factors;[16-18] limitating nitrogen in the culture medium induces trichothecene biosynthesis[19] and enhanced catabolism of specific amino acids negatively regulates trichothecene biosynthesis.[18] In addition, metals,[20, 21] polyamines,[22] ferulic acid,[23] and benzoxazinoids[24] have also been reported to affect trichothecene production by modulating *Tri6* expression. The effective concentrations of these substances were too high to assume their roles as molecules that bind specifically and tightly to a certain target protein and regulate the related signaling pathway in order to modulate *Tri6* expression.

From commercially available essential oils, Sakuda and co-workers isolated precocene II as an inhibitor of trichothecene production.[25] Distinct from other compounds, the effect of precocene II on trichothecene production was observed at low concentrations; it suppressed trichothecene production by 3-ADON-producing *F. graminearum* MAFF 101551 (strain H3) at low concentrations.[25] From this strain, a mitochondrial voltage-dependent anion channel (VDAC) was identified as a precocene II-binding protein using affinity magnetic beads.[26] In contrast to the sensitivity of trichothecene biosynthesis of strain MAFF 101551 to precocene II inhibition, mycotoxin production by strain JCM 9873 was not affected by this inhibitor.[27] Despite such clear differences, the amino acid sequences of the VDACs of these two strains were identical,[27] raising a question about the involvement of VDAC in the inhibition mechanism of trichothecene biosynthesis.

Specific inhibitors or activators of trichothecene biosynthesis are expected to serve as useful tools to unveil the molecular regulatory mechanisms underlying trichothecene biosynthesis. In addition, highly specific inhibitors are attractive compounds for developing more effective compounds to reduce mycotoxin contamination in the field.[28] We recently found that culturing on a 1-mL scale in 24-well plates stimulates trichothecene biosynthesis more effectively than by

maintaining the fungal culture conventionally in Erlenmeyer flasks. By using the 24-well plate culture method, we demonstrated that oligosaccharides containing an α-(1→2) (glucosyl/xylosyl)-fructosyl linkage act as inducer molecules of trichothecene biosynthesis for *F. graminearum*;[14] *i.e.*, sucrose induced trichothecene production not as a carbon source, but as an inducer effective at as low as 100 μM, a concentration applied to induce β-galactosidase in recombinant *Escherichia coli* by isopropyl-β-D-thiogalactopyranoside (IPTG). However, in contrast to IPTG, metabolizable sugars are very easily broken down to inactive monosaccharides by the action of hydrolytic enzymes secreted by the fungus.

In this study, through screening of the RIKEN Natural Product Depository (NPDepo) chemical library, we isolated compounds that modulate trichothecene production at several μM concentrations without inhibiting fungal growth. The influence of these compounds on *Tri* gene transcription was investigated.

RESULTS AND DISCUSSION

Screening for Chemicals That Modulate Trichothecene Biosynthesis Without Growth Inhibition. *F. graminearum* JCM 9873 was cultured in 1 mL of trichothecene-inducing YS_60 medium in a 24-well plate. The amount of 15-ADON was analyzed after incubation for 48 h in the presence of chemicals from RIKEN NPDepo library (final concentration of 10 μg mL^{-1} each). Among the 456 chemicals in the authentic and pilot libraries, two hit chemicals significantly altered 15-ADON production without adversely affecting *F. graminearum* growth (Table S1). Treatment with the library chemical NPD4346 (Figure 1), a synthetic furanocoumarin derivative, increased the amount of the trichothecene. Another chemical NPD4297 (Figure 1), a synthetic derivative of the antimalarial agent artemisinin, inhibited trichothecene production in the YS_60 culture.

Stimulation of Trichothecene Production by a Synthetic Furanocoumarin Derivative NPD12671. Twelve analogs of the hit chemical NPD4346 from the NPDepo chemical library, together with **1** (Figure 1) being the most common structure of these analogs, were tested for their ability to activate 15-ADON production. At 5 μg mL^{-1}, all compounds (Figure S1) except three, NPD4893, NPD4916, and **1**, stimulated trichothecene production in YS_60 medium in a 24-well plate (data not shown). Comparisons of the structures of these inactive chemicals to active ones with closest structures suggested that a propanamide moiety is indispensable for stimulation and that the *N*,*N*-dimethyl moiety of the side chain interrupts this stimulatory activity. In addition, attachment of a 2-methyl group, but not a 9-methyl group, to the linear furanocoumarin skeleton abolished the ability to activate trichothecene production (compare NPD4893 and NPD9811). As the stimulatory activities of the remaining 11 compounds were equally high in the YS_60 culture, trichothecene-non-inducing YG_60 medium was used to rank the activity of these chemicals (see below). From the result, we chose NPD12671 (Figure 1), one of the two compounds that showed the highest level of trichothecene production activation, for subsequent analysis (Figure S1 and Figure S2).

The effects of adding NPD12671 were investigated by using media with different levels of trichothecene-inducing activity. In sucrose-containing YS_60 medium that highly induces trichothecene biosynthesis,[29] 0.5 μM NPD12671 increased the amount of 15-ADON (per mycelial dry weight; MDW) by more than 2-fold upon 48 h of incubation (Figure 2). Accumulation of 15-ADON was further increased in the culture supplemented with 5 μM NPD12671, but the additional increase was rather limited. In trichothecene non-inducing YG_60 medium lacking sucrose, JCM 9873 did not produce detectable levels of 15-ADON at 48 h, as previously reported.[24] By adding 0.5 μM NPD12671 to the YG_60 culture, however, 15-ADON accumulation became detectable. Trichothecene production was more strongly activated by 5 μM NPD12671 (Figure 2).

At this concentration, a small amount of 15-ADON was produced by *F. graminearum*, even in nitrogen-rich YS_10 medium that does not induce trichothecene production.

NPD12671 and its analogs contain a psoralen structure, an unsubstituted linear furanocoumarin skeleton. Although psoralen itself shows photocarcinogenic properties, substituted psoralens exhibit decreased toxicity because they do not intercalate into DNA. As a structural core, they show a wide range of bioactive properties, such as anticancer, immunosuppressive, antipsoriasis, and antidiabetic activities, which are attributed to interactions of furanocoumarins with different biochemical targets.[30] In fact, psoralen and its derivatives bergapten and xanthotoxin suppress trichothecene production by weakly inhibiting Tri4p monooxygenase, thereby differing from the activity of NPD12671.[31] Such diverse effects displayed by this group of chemicals suggest the possibility of exploring their new biological activity through side chain modifications. Activation of microbial secondary metabolism may also be added to the list of unexploited furanocoumarin functions that draw the attention of chemical biologists.

NPD12671 Stimulates Trichothecene Production through Activation of *Tri6* Expression. To clarify the effect of NPD12671 on *Tri* gene transcription, we carried out northern blot analysis using RNA isolated from the 24-well plate culture of JCM 9873. In YS_60 medium, expressions of *Tri6*, *Tri5*, and *Tri4* were observed after 36 h of culturing; by adding 2 μM NPD12671, transcription of these *Tri* genes were upregulated to some extent (Figure 3). Differences in the mRNA levels of *Tri* genes between NPD12671-treated and -untreated cultures were more evident when the fungus was grown in YG_60 and YS_10 media, which do not induce trichothecene production without NPD12671. In addition, *Tri5* and *Tri4* expression was more strongly induced in the YG_60 culture than in the YS_10 culture upon treatment with NPD12671 (Figure 3), which is consistent with the amount of trichothecene that accumulated in each medium (Figure 2). However, the induction level of *Tri6* expression in the YG_60 culture was

equal to or slightly lower than that in the nitrogen-rich YS_10 culture (Figure 3), suggesting that nutrient conditions, such as nitrogen deficiency, are also important for NPD12671-mediated activation of *Tri5* and *Tri4*. In this way, the *Tri6* expression level does not always correlate with the level of pathway *Tri* genes that are positively regulated by the Tri6p transcription factor.

Inhibition of Trichothecene Production by Artemisinin Derivatives. The hit chemical NPD4297 is a synthetic artemisinin derivative that contains an L-leucyl-L-threonine dipeptide amide bonded to the artemisinin skeleton through a hemisuccinate linker (Figure 1). To search for more potent inhibitors of trichothecene biosynthesis, 12 analogs of NPD4297 from the NPDepo chemical library (Figure S3) were tested for their ability to suppress 15-ADON accumulation in YS_60 culture in a 24-well plate. Among these artemisinin analogs, 5 compounds showed more potent inhibitory action against trichothecene production at 1 μg mL^{-1} (Figure S3), including NP28 of dihydroartemisinin (DHA) (Figure 1), a hemiacetal derivative of artemisinin where the C-10 ketone was reduced to a hydroxyl group. None of these library compounds affected *F. graminearum* growth at this concentration. As the activity of DHA was comparable to that of the other 4 analogs, we chose commercially available DHA for further analysis.

In addition to DHA, the parent natural product artemisinin and its synthetic derivatives artesunate (ATS), a hemisuccinyl ester derivative of DHA, and artemether (ATM), a methyl ether derivative of DHA, are also commercially available at affordable costs. Thus, we evaluated the inhibitory activities of these analogs against the YS_60 culture in a 24-well plate. Among these artemisinin derivatives, DHA most effectively inhibited trichothecene production after 48 h of culture (Figure 4). Upon treatment with 1 μM (0.28 μg mL^{-1}) of DHA, the amount of 15-ADON significantly decreased ($P < 0.05$). Similarly, ATS showed inhibitory activity against trichothecene production; a significant decrease ($P < 0.01$) in the amount of 15-ADON was observed at 2 μM (0.77

μg mL^{-1}). These two synthetic artemisinin derivatives completely inhibited trichothecene production at 5 μM under the culture conditions used. Upon ATM treatment, the necessary concentration to detect statistical significance ($P < 0.05$) increased to 5 μM (1.49 μg mL^{-1}). The inhibitory activity of artemisinin was similarly as low as that of ATM; trichothecene production could not be completely inhibited at 5 μM (Figure S4). Given that a succinate ester, but not *O*-methyl and keto groups, is biologically labile and can be hydrolyzed in fungal cells, a free hydroxyl at C-10 appears to be an important functional group for inhibiting trichothecene production.

The artemisinin analog DHA showed varying inhibitory action against trichothecene production in other strains with different chemotypes, such as MAFF 240560 and MAFF 101551, but did not inhibit production in MAFF 240548, even at 20 μM (Figure S5). Although the molar concentration of DHA necessary for inhibiting trichothecene biosynthesis was two orders of magnitude lower than that of the previously identified inhibitor 2,4-dihydroxy-7-methoxy-2*H*-1,4-benzoxazin-3(4*H*)-one (DIMBOA),[24] the relative insensitivity of the NIV-chemotype strain MAFF 240548 to exogenous compounds was similarly observed with this strain. This may be attributed to a higher ability of this strain to metabolize or transport xenobiotics out of the cells.

DHA Inhibits Trichothecene Production through Repression of *Tri6* Transcription. To clarify the mode of action of DHA on trichothecene biosynthesis, a time course of *Tri* gene expression was investigated using mycelia grown in trichothecene-inducing YS_60 medium. Northern blot analysis revealed that DHA treatment (5 μM) strongly inhibited transcription of *Tri6* at 48 h and 60 h, corresponding with the time that *Tri6* mRNA accumulates at high levels in the untreated fungus (Figure 5). As expected from the *Tri6* transcript level, the amount of *Tri4* and *Tri5* mRNAs was marginal in the DHA-treated cells at these time points. This result suggests that at least one action site of DHA is in the signal transduction pathway leading to activation of *Tri6* transcription.

Effects of the Chemicals on Mycelial Pigmentation. While investigating the effects of NPD12671 and DHA on trichothecene production, we noticed that these two chemicals differently impacted pigmentation of the mycelia. As shown in Figure S6, NPD12671 caused severe albinism at 1 μM, but DHA, on the contrary, led to browning of the mycelia in a dose dependent manner (Figure S6). As *F. graminearum* produces red pigment aurofusarin that gives a yellow color in acidic conditions,[32] we examined whether the chemical treatments affected expression of the *PKS12* gene (FGSG_02324) required for aurofusarin biosynthesis.[33] As speculated, 2 μM NPD12671 suppressed accumulation of *PKS12* mRNA on northern blots (Figure S6). However, transcription of *PKS12* was not affected by treatment with 5 μM DHA (Figure S6). Comparative LC-MS/MS analyses of possible *F. graminearum* secondary metabolites (*i.e.*, aurofusarin, fusarielin H, fusarin C, zearalenone)[17, 34] in the presence and absence of these chemicals may unveil global effects of these chemicals on secondary metabolite biosynthesis.

Identifying Culture Conditions under Which DHA Inhibits Trichothecene Production in a Constitutive *Tri6* Overexpressor. As the expression level of *Tri6* was not always correlated with that of pathway *Tri* genes (Figure 3), it may be possible that functional modulation of Tri6p or other regulatory factor(s) also serves to inhibit trichothecene biosynthesis upon DHA treatment. We thus sought to determine whether the inhibition occurs without transcriptional repression of *Tri6* by identifying culture conditions under which most pathway *Tri* genes are transcriptionally repressed but a large amount of *Tri6* mRNA exists. For this purpose, we generated a *Tri6* overexpressor strain by transforming strain JCM 9873 with an ectopic integration vector pTef-Tri6-hph (Figure S7), which contains *Tri6* under the control of a constitutive *TEF* promoter from *Aspergillus nidulans*.[29] From 12 hygromycin B-resistant colonies, one transformant, *Tri6*$^{O/E}$ #2s1 (Figure S7), was selected as a constitutive overexpressor with the highest level of 15-ADON production. Compared to the wild-type, the

overexpressor *Tri6*$^{O/E}$ #2s1 produced an increased amount of 15-ADON in YS_60 medium by the 24-well plate culture method, which was not decreased by the addition of 5 μM DHA (Figure S8a). The inability of DHA to inhibit mycotoxin production by *Tri6*$^{O/E}$ #2s1 contrasts with its inhibitory action against the wild-type strain, in which the initial activation of *Tri6* expression in the YS_60 culture was suppressed as demonstrated by northern blot analysis (Figure 5).

Upon growth in YG_60 medium distributed in 24-well plates, the wild-type strain failed to produce trichothecenes (data not shown) as previously reported.[14] In contrast, this overexpressor strain accumulated a considerable amount of 15-ADON in the YG_60 culture (Figure S8b; upper panel). Similar to the case with the YS_60 culture (Figure S8a; lower panel), the addition of 5 μM DHA to YG_60 medium did not essentially affect trichothecene production by the overexpressor. When the overexpressor was grown on a 30-mL scale using a 100-mL Erlenmeyer flask, 15-ADON accumulated in the YS_60 culture, and to a much lesser extent, in the YG_60 culture (Figure S8b; lower panel). While adding 5 μM DHA to the YS_60 medium did not significantly alter the amount of 15-ADON, trichothecene production was significantly reduced in the YG_60 flask culture, where the induction of trichothecene biosynthesis was weaker than biosynthesis upon culture in 24-well plates. Upon DHA treatment, an extremely weak blue spot of 15-ADON was hardly visible on a TLC plate of the YG_60 culture extract (Figure S8b; lower panel).

Additional Factor(s) Modulated by DHA Are Necessary for Transcriptional Activation of Pathway *Tri* Genes. By using RNA isolated from the mycelia of the overexpressor grown in Erlenmeyer flasks, we examined a time course of *Tri* gene expression. In the YG_60 culture supplemented with 5 μM DHA, expression of *Tri6* from both native and constitutive *TEF* promoters remained constant throughout the incubation period. In contrast, the concentrations of *Tri5* and *Tri4* transcripts were considerably decreased upon 36 h of incubation with DHA (Figure 6). Although the

transcript levels gradually increased over the incubation period, the total sum of the temporal expression level (integral of time and transcript level) was still much lower compared to that of the untreated control. This result reasonably explains the extremely limited accumulation of 15-ADON in the DHA-treated culture (Figure S8b; lower panel). Since the abundance of Tri6p is constantly kept at a high level in the overexpressor, DHA might have negatively modulated activities of some additional component(s) in the absence of sucrose, *e.g.*, Tri10p, transcriptional coactivators that physically interact with Tri6p, or enzymes that post-translationally modify Tri6p, that are necessary for transcriptional activation of pathway *Tri* genes. Perhaps the quality and quantity of such factor(s) are also regulated by the sugars in the medium.[14] In contrast to the dependency of pathway *Tri* gene expression on such component(s), Tri6p-independent initial activation of *Tri6* expression appears to depend to a much lesser extent on trichothecene-specific coactivator(s); indeed, a recombinant *F. graminearum* strain in which non-sense mutations were introduced into *Tri6* (*Tri6_nsm*) and *Tri10* (*Tri10_nsm*) still showed expression of a small amount of the *Tri6_nsm* transcript but not the *Tri5* transcript from the native locus of the trichothecene gene cluster (our preliminary unpublished results). In any case, repression of initial activation of *Tri6* expression is not the only point of DHA's inhibitory action against trichothecene production under the culture conditions tested.

The Trichothecene Production-modulating Activities of NPD12671 and DHA Are Also Effective on the Δ*FgOs2* Mutant. A previous study revealed the involvement of FgOS2 mitogen-activated protein kinase (MAPK), an ortholog of yeast Hog1 MAPK, in the biosynthesis of NIV-type trichothecenes.[35] To determine whether the Hog1 MAPK cascade mediated the activities of NPD12671 and DHA, we generated FgOS2 disruption mutants in strain JCM 9873, Δ*FgOs2* (Figure S9), and examined the effect of these chemicals on trichothecene production. When the Δ*FgOs2* mutant strains Δ*os2* #1 and #9 were treated with 1 μM NPD12671, 15-ADON production was

significantly activated, as was observed in the wild-type strain (Figure 7; upper panel). By increasing the culture period from 48 h to 96 h, the fungal mass of the mutant culture, but not the wild-type culture, was statistically reduced to some extent by treatment with 1 μM NPD12671. However, 15-ADON production by the mutant reached equal levels to those of the wild-type culture. These results indicate that the activation was not mediated by FgOS2 function; NPD12671 may target downstream components of the Hog1 MAPK pathway or other factors involved in regulating *Tri6* transcription. Similar to the case of NPD12671, DHA also modulated trichothecene biosynthesis in the Δ*FgOs2* strains. However, the activity of DHA was more pronounced in the Δ*FgOs2* strains; at 48 h, 15-ADON production was completely inhibited by the mutation in the presence of 1 μM DHA, at which concentration the treated wild-type strain produced a considerable amount of the mycotoxin (Figure 7; lower panel). At 96 h of incubation, the inhibition of trichothecene accumulation was markedly alleviated in the wild-type strain. Against the mutant strains, however, the inhibitory activity remained at a high level. Thus, DHA appears to act on signaling pathway(s) other than the Hog1 MAPK pathway to activate trichothecene biosynthesis.

To determine the interactive relationships of NPD12671 and DHA on trichothecene production, the fungal culture was supplemented with both compounds at different concentrations. Although their effects were competitive (Figure S10), the outcome of simultaneous activation and inhibition treatments depended on the strains (and perhaps on culture conditions); the amount of DHA necessary to completely abrogate trichothecene production in the culture supplemented with 1 μM NPD12671 was 2 μM for the Δ*FgOs2* mutant, but even 10 μM DHA was not sufficient for the wild-type strain. The difference in efficiencies of these compounds to modulate trichothecene production suggests that they may act on different regulatory pathways of trichothecene biosynthesis.

Miscellaneous Properties of DHA against *F. graminearum.* Based on the available knowledge on the growth inhibitory action of artemisinins against yeast, we first questioned whether DHA-mediated inhibition of trichothecene biosynthesis is associated with a mitochondrial mechanism (see Background Information in the Supporting Information). Fungal mitochondria harbor external NADH dehydrogenases that oxidize NADH at the cytosolic side (intermembrane space) of the inner membrane, in addition to the internal NADH dehydrogenases (and classical complex I of the electron transport chain in many fungi) responsible for oxidizing NADH in the matrix.[36] In yeast, a single gene disruption of *NDE1*, which encodes an external NADH dehydrogenase, ameliorates growth defects caused by artemisinins on non-fermentable (mitochondrial respiration-dependent) media. To see if trichothecene biosynthesis inhibition by DHA was mediated through reducing the endoperoxide moiety by the function of Nde1p,[36] we disrupted the *F. graminearum* ortholog of this gene, *FgNde1* (FGSG_04130), by double cross-over homologous recombination. When assayed by the 24-well plate culture method, DHA equally inhibited trichothecene biosynthesis in the wild-type and Δ*FgNde1* mutant (Figure S11). Although the metabolic fates of DHA and its biochemical and physiological effects on the mitochondria remain to be investigated, the result suggests that DHA has a mitochondria-independent mode of action.

Since the exogenous addition of hydrogen peroxide (H_2O_2) accelerated *Tri* gene expression at an early culture stage of strain CBS185.32,[37] it was hypothesized that oxidative stress caused by H_2O_2 triggers trichothecene biosynthesis and increases final trichothecene yield. Although exogenously added 0.5 mM H_2O_2 did not activate 15-ADON biosynthesis in strain JCM 9873 (data not shown) in contrast to findings of a previous report,[37] this may be attributed to differences of the detoxification ability of each fungal strain in response to exogenously added reactive oxygen species (ROS). We thus investigated whether the cellular level of ROS at an early stage of JCM 9873 culture correlates with the inhibitory and stimulatory effects of DHA and NPD12671,

respectively, on trichothecene production. When the young mycelia in YS_60 medium were treated with the H_2O_2-specific fluorescent dye BES-H_2O_2-Ac, the intracellular H_2O_2 was visualized as green fluorescence under epifluorescence microscopy (Figure 8a upper panels). The addition of 5 μM DHA and 1 μM NPD12671 attenuated and strengthened the fluorescence, respectively, suggesting that intracellular H_2O_2 level was also altered as such by the chemicals. Furthermore, DHA stimulated generation of the superoxide anion that is known to suppress trichothecene production,[37] as demonstrated by enhanced green fluorescence of the mycelia treated with the superoxide anion-specific fluorescent dye BES-So-AM (Figure 8b upper panels). These results indicate that ROS may modulate trichothecene biosynthesis by the compounds tested. However, H_2O_2 concentration did not always correlate with the amount of 15-ADON, as the Δ*FgOs2* mutant showed very bright fluorescence (Figure 8a lower panels). Thus, an appropriate level of intracellular ROS may be important for initiating trichothecene biosynthesis. Alternatively, H_2O_2 is necessary but not sufficient for stimulating trichothecene biosynthesis; other necessary factors may be the determinant for the Δ*FgOs2* mutant. The positive effect of DHA on reducing H_2O_2 level appears to be a general property of the compound under trichothecene-producing conditions, as treatment of the Δ*FgOs2* mutant with DHA also suppressed intracellular H_2O_2 generation.

Conclusion and Perspectives. From the NPDepo chemical library, we identified compounds that modulate trichothecene production by *F. graminearum*: a linear furanocoumarin NPD12671 and artemisinin analog DHA activated and inhibited trichothecene production, respectively, in a strain-specific manner. As previously demonstrated by the lethal effect of artemisinin against yeast, at least two different targets for the inhibitory action of DHA were suggested to exist in pathways leading to trichothecene biosynthesis. Although identifying specific molecular targets of these compounds was beyond the scope of this investigation, inhibition analysis using DHA

convinced us of the importance of molecular genetic studies that allow discrimination between Tri6p-independent initial activation of *Tri6* expression and subsequent Tri6p-dependent activation of *Tri* gene expression.

METHODS

Strains, Media, and Main Culture for Trichothecene Production Assay. *F. graminearum* JCM 9873, a 15-ADON chemotype, was used in this study, unless otherwise noted. The transformants and wild-type strains were maintained on V8 juice agar[24] with or without 300 μg mL^{-1} hygromycin B, respectively. Conidia were induced by inoculating the mycelial plug into the carboxymethylcellulose medium as described previously.[24]

To prepare fresh inoculum for the main culture, conidial suspensions were inoculated into YG medium (2% glucose, 0.5% Bacto™ yeast extract; Becton, Dickinson and Company) at a final concentration of 1×10^4 mL^{-1} and allowed to germinate with reciprocal shaking at 125 rpm and 25°C for 16 h–24 h. The germinated spores (pre-culture) were then diluted 100-fold in one of the following media: YS_60 medium (6% sucrose, 0.1% Bacto™ yeast extract), YS_10 medium (6% sucrose, 0.6% Bacto™ yeast extract), YG_60 medium (6% glucose, 0.1% Bacto™ yeast extract), and YG_10 medium (6% glucose, 0.6% Bacto™ yeast extract).

Screening of Chemicals That Affect Trichothecene Accumulation in YS_60 Medium. To screen for chemicals that affect trichothecene synthesis, 1-mL aliquots of the YS_60 culture were distributed into 24-well plates (VTC-24, AS ONE) and supplemented with 10 μg mL^{-1} of each library compound. After 48 h of incubation with gyratory shaking at 135 rpm and 25°C, a 600-μL aliquot of the culture supernatant from each well was extracted with an equal volume of ethyl acetate, the solvent was evaporated under a gentle stream of nitrogen, and the metabolites were analyzed by thin layer chromatography (TLC) as described in Supporting Information.

Culturing of *F. graminearum* for RNA Analysis. To evaluate the effects of NPD12671 (Figure 3) and DHA (Figure 5) on *Tri* gene expression, 1-mL aliquots of the wild-type culture were distributed into 24-well plates. For the *Tri6* overexpressor (Figure 6), 30-mL aliquots of the YG_60 culture were transferred to 100-mL Erlenmeyer flasks. The cultures were incubated with or without the compound with gyratory shaking at 135 rpm and 25°C. After the desired incubation period, twenty 1-mL aliquots of the 24-well plate culture or five 4-mL aliquots of the 100-mL Erlenmeyer flask culture were sampled and combined; the cultures remaining in the flasks were further incubated until the last sampling time. At each sampling time, the mycelia were collected by filtration through Miracloth (Merck Millipore) and used for RNA preparation.

ASSOCIATED CONTENT

Supporting Information

The Supporting Information is available free of charge on the ACS Publications website at DOI: .

Background information, additional details of methods, two tables, and eleven figures of additional data (PDF)

AUTHOR INFORMATION

Corresponding Author

*E-mail: mkimura@agr.nagoya-u.ac.jp

ORCID

Kazuyuki Maeda: 0000-0003-1015-9499

Yuichi Nakajima: 0000-0003-0318-2527

Kyoko Kanamaru: 0000-0003-3964-7891

Tetsuo Kobayashi: 0000-0002-4008-454X

Takumi Nishiuchi: 0000-0001-9429-5396

Hiroyuki Osada: 0000-0002-3606-4925

Makoto Kimura: 0000-0001-5310-2893

Notes

The authors declare no competing financial interest.

ACKNOWLEDGEMENTS

This work was supported by the Program for Promotion of Basic Research Activities for Innovative Biosciences (PROBRAIN) and a Noda Institute for Scientific Research grant (2015). We thank T. Saito in the RIKEN NPDepo for providing compounds.

REFERENCES

(1) Kimura, M., Tokai, T., Takahashi-Ando, N., Ohsato, S., and Fujimura, M. (2007) Molecular and genetic studies of *Fusarium* trichothecene biosynthesis: pathways, genes, and evolution. *Biosci. Biotechnol. Biochem. 71*, 2105-2123.

(2) McCormick, S. P., Stanley, A. M., Stover, N. A., and Alexander, N. J. (2011) Trichothecenes: from simple to complex mycotoxins. *Toxins 3*, 802-814.

(3) Pestka, J. J., and Smolinski, A. T. (2005) Deoxynivalenol: toxicology and potential effects on humans. *J. Toxicol. Environ. Health B Crit. Rev. 8*, 39-69.

(4) Brown, D. W., McCormick, S. P., Alexander, N. J., Proctor, R. H., and Desjardins, A. E. (2002) Inactivation of a cytochrome P-450 is a determinant of trichothecene diversity in *Fusarium* species. *Fungal Genet. Biol. 36*, 224-233.

(5) Lee, T., Oh, D. W., Kim, H. S., Lee, J., Kim, Y. H., Yun, S. H., and Lee, Y. W. (2001) Identification of deoxynivalenol- and nivalenol-producing chemotypes of *Gibberella zeae* by using PCR. *Appl. Environ. Microbiol. 67*, 2966-2972.

(6) Kimura, M., Tokai, T., O'Donnell, K., Ward, T. J., Fujimura, M., Hamamoto, H., Shibata, T., and Yamaguchi, I. (2003) The trichothecene biosynthesis gene cluster of *Fusarium graminearum* F15 contains a limited number of essential pathway genes and expressed non-essential genes. *FEBS Lett. 539*, 105-110.

(7) Hohn, T. M., and Beremand, P. D. (1989) Isolation and nucleotide sequence of a sesquiterpene cyclase gene from the trichothecene-producing fungus *Fusarium sporotrichioides*. *Gene 79*, 131-138.

(8) McCormick, S. P., Alexander, N. J., and Proctor, R. H. (2006) *Fusarium Tri4* encodes a multifunctional oxygenase required for trichothecene biosynthesis. *Can. J. Microbiol. 52*, 636-642.

(9) Tokai, T., Koshino, H., Takahashi-Ando, N., Sato, M., Fujimura, M., and Kimura, M. (2007) *Fusarium Tri4* encodes a key multifunctional cytochrome P450

monooxygenase for four consecutive oxygenation steps in trichothecene biosynthesis. *Biochem. Biophys. Res. Commun. 353*, 412-417.

(10) Desjardins, A. E., Hohn, T. M., and McCormick, S. P. (1993) Trichothecene biosynthesis in *Fusarium* species: chemistry, genetics, and significance. *Microbiol. Rev. 57*, 595-604.

(11) Proctor, R. H., Hohn, T. M., McCormick, S. P., and Desjardins, A. E. (1995) *Tri6* encodes an unusual zinc finger protein involved in regulation of trichothecene biosynthesis in *Fusarium sporotrichioides*. *Appl. Environ. Microbiol. 61*, 1923-1930.

(12) Seong, K. Y., Pasquali, M., Zhou, X., Song, J., Hilburn, K., McCormick, S., Dong, Y., Xu, J. R., and Kistler, H. C. (2009) Global gene regulation by *Fusarium* transcription factors *Tri6* and *Tri10* reveals adaptations for toxin biosynthesis. *Mol. Microbiol. 72*, 354-367.

(13) Tag, A. G., Garifullina, G. F., Peplow, A. W., Ake, C., Jr., Phillips, T. D., Hohn, T. M., and Beremand, M. N. (2001) A novel regulatory gene, *Tri10*, controls trichothecene toxin production and gene expression. *Appl. Environ. Microbiol. 67*, 5294-5302.

(14) Nakajima, Y., Maeda, K., Jin, Q., Takahashi-Ando, N., Kanamaru, K., Kobayashi, T., and Kimura, M. (2016) Oligosaccharides containing an α-(1→2) (glucosyl/xylosyl)-fructosyl linkage as inducer molecules of trichothecene biosynthesis for *Fusarium graminearum*. *Int. J. Food Microbiol. 238*, 215-221.

(15) Gardiner, D. M., Osborne, S., Kazan, K., and Manners, J. M. (2009) Low pH regulates the production of deoxynivalenol by *Fusarium graminearum*. *Microbiology 155*, 3149-3156.

(16) Min, K., Shin, Y., Son, H., Lee, J., Kim, J. C., Choi, G. J., and Lee, Y. W. (2012) Functional analyses of the nitrogen regulatory gene *areA* in *Gibberella zeae*. *FEMS Microbiol. Lett. 334*, 66-73.

(17) Giese, H., Sondergaard, T. E., and Sørensen, J. L. (2013) The AreA transcription factor in *Fusarium graminearum* regulates the use of some nonpreferred nitrogen sources and secondary metabolite production. *Fungal Biol. 117*, 814-821.

(18) Maeda, K., Nakajima, Y., Tanahashi, Y., Kitou, Y., Miwa, A., Kanamaru, K., Kobayashi, T., Nishiuchi, T., and Kimura, M. (2017) L-Threonine and its analogue added to autoclaved solid medium suppress trichothecene production by *Fusarium graminearum*. *Arch. Microbiol. 199*, 945-952.

(19) Miller, J. D., and Blackwell, B. A. (1986) Biosynthesis of 3-acetyldeoxynivalenol and other metabolites by *Fusarium culmorum* HLX 1503 in a stirred jar fermentor. *Can. J. Bot. 64*, 1-5.

(20) Pinson-Gadais, L., Richard-Forget, F., Frasse, P., Barreau, C., Cahagnier, B., Richard-Molard, D., and Bakan, B. (2008) Magnesium represses trichothecene biosynthesis and modulates *Tri5*, *Tri6*, and *Tri12* genes expression in *Fusarium graminearum*. *Mycopathologia 165*, 51-59.

(21) Tsuyuki, R., Yoshinari, T., Sakamoto, N., Nagasawa, H., and Sakuda, S. (2011) Enhancement of trichothecene production in *Fusarium graminearum* by cobalt chloride. *J. Agric. Food Chem. 59*, 1760-1766.

(22) Gardiner, D. M., Kazan, K., and Manners, J. M. (2009) Nutrient profiling reveals potent inducers of trichothecene biosynthesis in *Fusarium graminearum*. *Fungal Genet. Biol. 46*, 604-613.

(23) Boutigny, A. L., Barreau, C., Atanasova-Penichon, V., Verdal-Bonnin, M. N., Pinson-Gadais, L., and Richard-Forget, F. (2009) Ferulic acid, an efficient inhibitor of type B trichothecene biosynthesis and *Tri* gene expression in *Fusarium* liquid cultures. *Mycol. Res. 113*, 746-753.

(24) Etzerodt, T., Maeda, K., Nakajima, Y., Laursen, B., Fomsgaard, I. S., and Kimura, M. (2015) 2,4-Dihydroxy-7-methoxy-2*H*-1,4-benzoxazin-3(4*H*)-one (DIMBOA)

inhibits trichothecene production by *Fusarium graminearum* through suppression of *Tri6* expression. *Int. J. Food Microbiol. 214*, 123-128.

(25) Yaguchi, A., Yoshinari, T., Tsuyuki, R., Takahashi, H., Nakajima, T., Sugita-Konishi, Y., Nagasawa, H., and Sakuda, S. (2009) Isolation and identification of precocenes and piperitone from essential oils as specific inhibitors of trichothecene production by *Fusarium graminearum*. *J. Agric. Food Chem. 57*, 846-851.

(26) Furukawa, T., Sakamoto, N., Suzuki, M., Kimura, M., Nagasawa, H., and Sakuda, S. (2015) Precocene II, a trichothecene production inhibitor, binds to voltage-dependent anion channel and increases the superoxide level in mitochondria of *Fusarium graminearum*. *PLoS One 10*, e0135031.

(27) Maeda, K., and Ohsato, S. (2017) Molecular genetic characterization of *Fusarium graminearum* genes identified as encoding a precocene II-binding protein. *JSM Mycotoxins 67*, 1-3.

(28) Maeda, K., Nakajima, Y., Motoyama, T., Kondoh, Y., Kawamura, T., Kanamaru, K., Ohsato, S., Nishiuchi, T., Yoshida, M., Osada, H., Kobayashi, T., and Kimura, M. (2017) Identification of a trichothecene production inhibitor by chemical array and library screening using trichodiene synthase as a target protein. *Pestic. Biochem. Physiol. 138*, 1-7.

(29) Nakajima, Y., Tokai, T., Maeda, K., Tanaka, A., Takahashi-Ando, N., Kanamaru, K., Kobayashi, T., and Kimura, M. (2014) A set of heterologous promoters useful for investigating gene functions in *Fusarium graminearum*. *JSM Mycotoxins 64*, 147-152.

(30) Shalaby, N. M., Abd-Alla, H. I., Aly, H. F., Albalawy, M. A., Shaker, K. H., and Bouajila, J. (2014) Preliminary *in vitro* and *in vivo* evaluation of antidiabetic activity of *Ducrosia anethifolia* Boiss. and its linear furanocoumarins. *Biomed. Res. Int. 2014*, 480545.

(31) Takahashi-Ando, N., Ochiai, N., Tokai, T., Ohsato, S., Nishiuchi, T., Yoshida, M., Fujimura, M., and Kimura, M. (2008) A screening system for inhibitors of

trichothecene biosynthesis: hydroxylation of trichodiene as a target. *Biotechnol. Lett. 30*, 1055-1059.

(32) Shibata, S., Morishita, E., Takeda, T., and Sakata, K. (1968) Metabolic products of fungi. XXVIII. The Structure of aurofusarin. (1). *Chem. Pharm. Bull. 16*, 405-410.

(33) Kim, J. E., Han, K. H., Jin, J., Kim, H., Kim, J. C., Yun, S. H., and Lee, Y. W. (2005) Putative polyketide synthase and laccase genes for biosynthesis of aurofusarin in *Gibberella zeae*. *Appl. Environ. Microbiol. 71*, 1701-1708.

(34) Droce, A., Sørensen, J. L., Sondergaard, T. E., Rasmussen, J. J., Lysøe, E., and Giese, H. (2017) PTR2 peptide transporters in *Fusarium graminearum* influence secondary metabolite production and sexual development. *Fungal Biol. 121*, 515-527.

(35) Ochiai, N., Tokai, T., Nishiuchi, T., Takahashi-Ando, N., Fujimura, M., and Kimura, M. (2007) Involvement of the osmosensor histidine kinase and osmotic stress-activated protein kinases in the regulation of secondary metabolism in *Fusarium graminearum*. *Biochem. Biophys. Res. Commun. 363*, 639-644.

(36) Sun, C., and Zhou, B. (2016) The molecular and cellular action properties of artemisinins: what has yeast told us? *Microb. Cell 3*, 196-205.

(37) Ponts, N., Pinson-Gadais, L., Verdal-Bonnin, M. N., Barreau, C., and Richard-Forget, F. (2006) Accumulation of deoxynivalenol and its 15-acetylated form is significantly modulated by oxidative stress in liquid cultures of *Fusarium graminearum*. *FEMS Microbiol. Lett. 258*, 102-107.

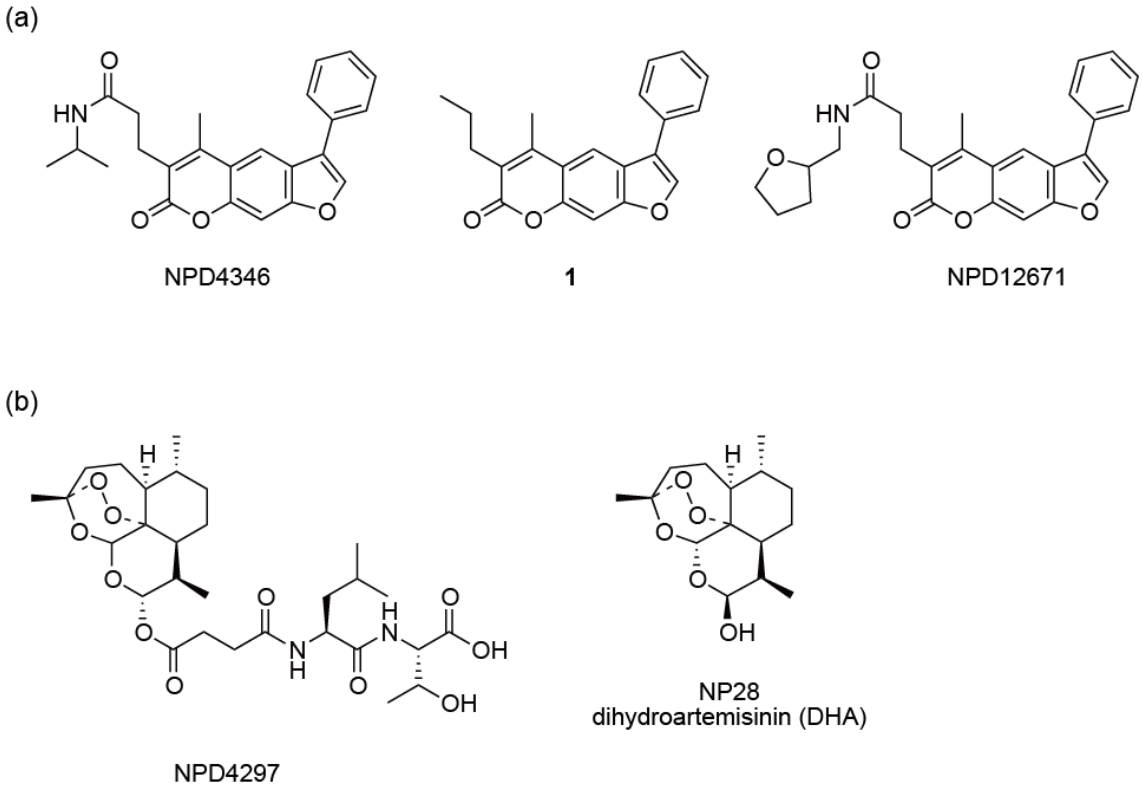

Figure 1. Chemical structures of key hit chemicals described in this paper. (a) Synthetic furanocoumarin derivatives. NPD4346 was originally identified as an activator of trichothecene biosynthesis from the library. Among the analogs with a common basic skeleton (**1**) included in the NPDepo chemical library, NPD12671 activated trichothecene biosynthesis in *F. graminearum* JCM 9873 most strongly. (b) Artemisinin derivatives. NPD4297 was originally identified as an inhibitor of trichothecene biosynthesis from the library. Among the commercially available artemisinin analogs, DHA inhibited trichothecene biosynthesis in *F. graminearum* JCM 9873 most strongly.

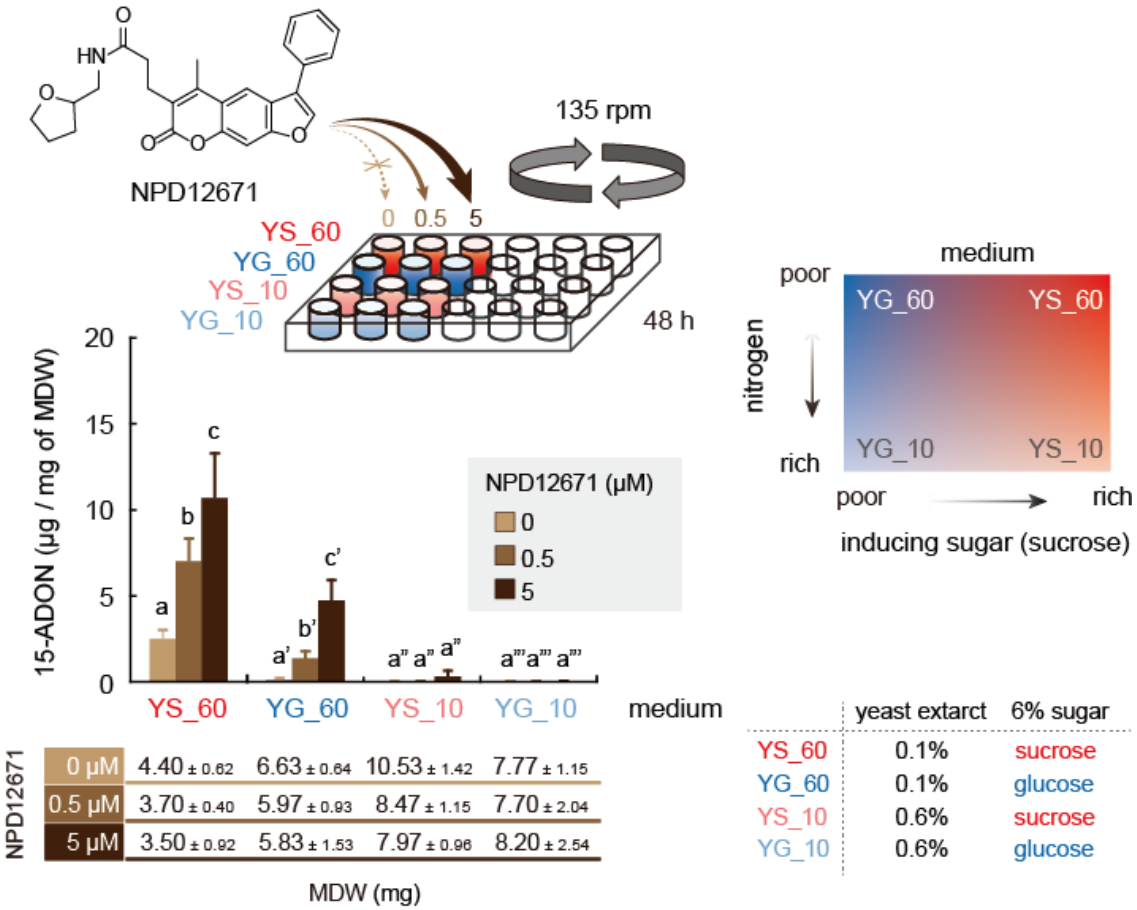

Figure 2. Stimulatory activity of a synthetic furanocoumarin derivative NPD12671 on trichothecene production by *F. graminearum* JCM 9873. Pre-cultures of germinated spores were transferred to various media with different degrees of trichothecene production-inducing activities. The inoculum was then distributed into 24-well plates and treated with NPD12671 at the concentrations as indicated. After 48 h of incubation, the amount of 15-ADON was quantified. Data were obtained from triplicate experiments, each using an independent pre-culture. Different letters indicate significant differences determined by one-way ANOVA followed by Tukey-Kramer test ($P < 0.05$).

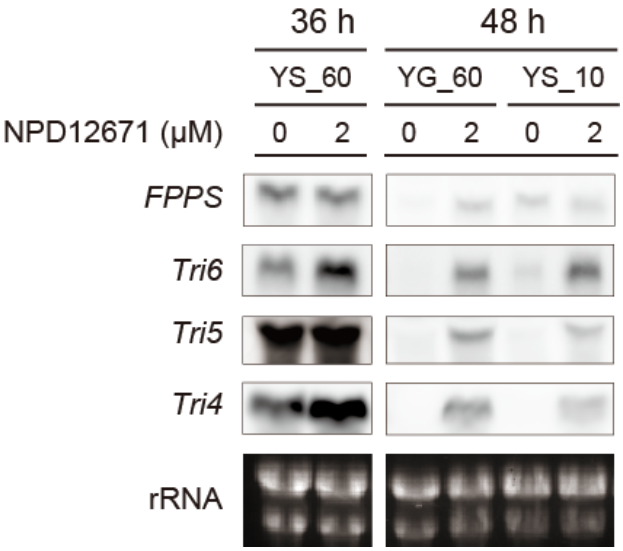

Figure 3. Northern blot analysis of RNA isolated from *F. graminearum* JCM 9873 cultured in YS_60, YG_60, and YS_10 media. The fungus was grown with or without 2 μM NPD12671 in a 24-well plate. Ten micrograms of total RNA were hybridized with DIG-labeled DNA probes for *FPPS* (FPP synthase gene; FGSG_06784), *Tri6*, *Tri5*, and *Tri4*. The formaldehyde gel stained with ethidium bromide is shown below each lane to demonstrate equal RNA loading.

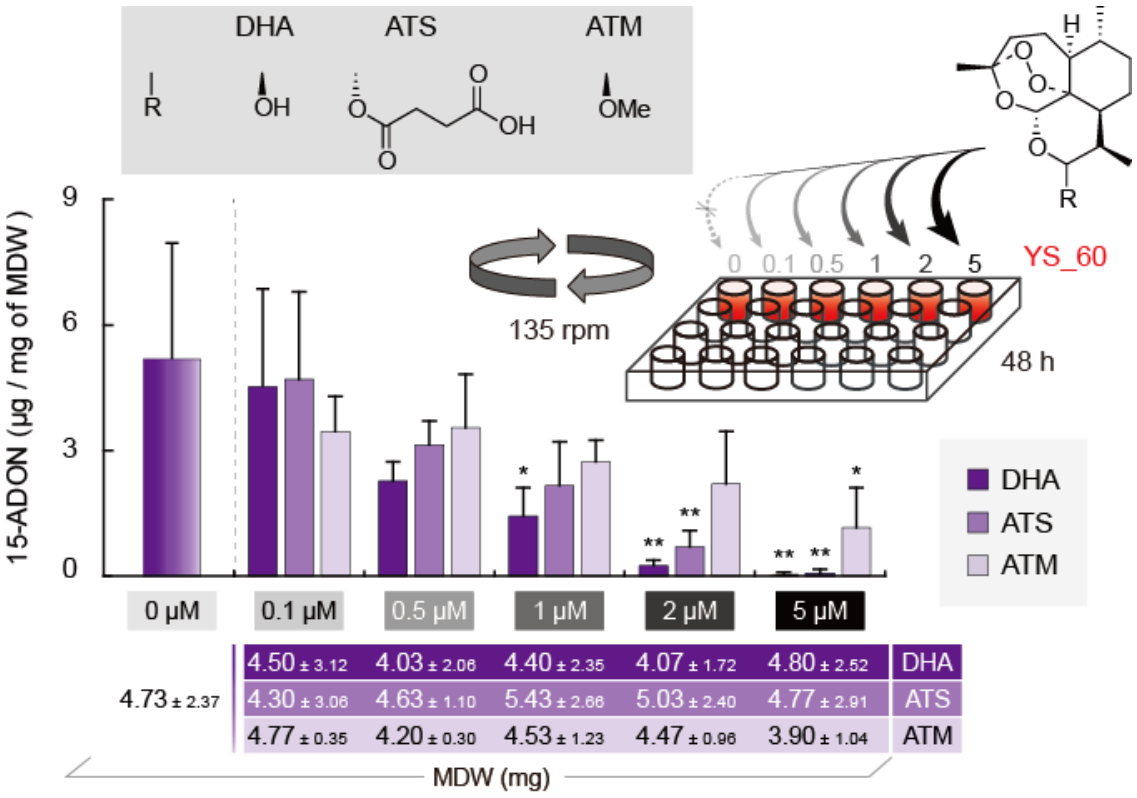

Figure 4. Inhibitory activity of artemisinin derivatives on trichothecene production by *F. graminearum* JCM 9873. Germinated spores (pre-culture) were inoculated into YS_60 medium and distributed into 24-well plates. Artemisinin analogs, DHA, ATS, and ATM, were added to the YS_60 culture at various concentrations as indicated. After 48 h of incubation, the amount of 15-ADON was quantified. Data were obtained from triplicate experiments using three independent pre-culture preparations. Asterisks indicate significant differences between control (0 μM) and treated (0.1–5 μM) cultures determined by one-way ANOVA followed by Dunnett's multiple comparison test (*P < 0.05, **P < 0.01).

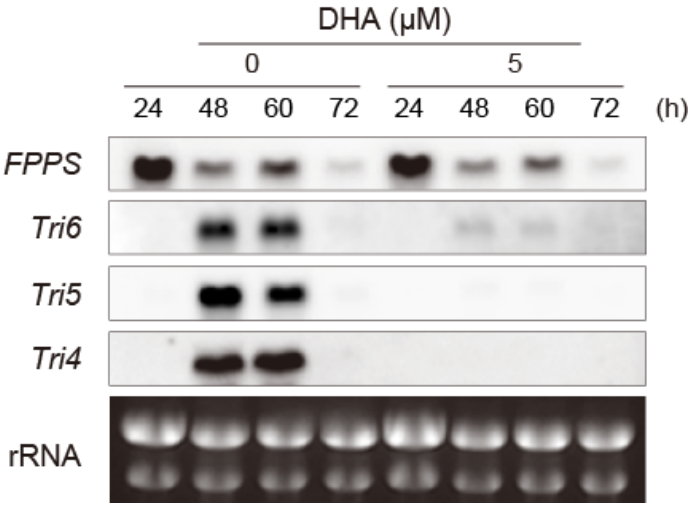

Figure 5. Northern blot analysis of RNA isolated from YS_60 culture of *F. graminearum* JCM 9873 in a 24-well plate with or without 5 μM DHA treatment. Ten micrograms of total RNA were hybridized with DIG-labeled DNA probes for *FPPS*, *Tri6*, *Tri5*, and *Tri4*. The formaldehyde gel stained with ethidium bromide is shown below each lane to demonstrate equal RNA loading.

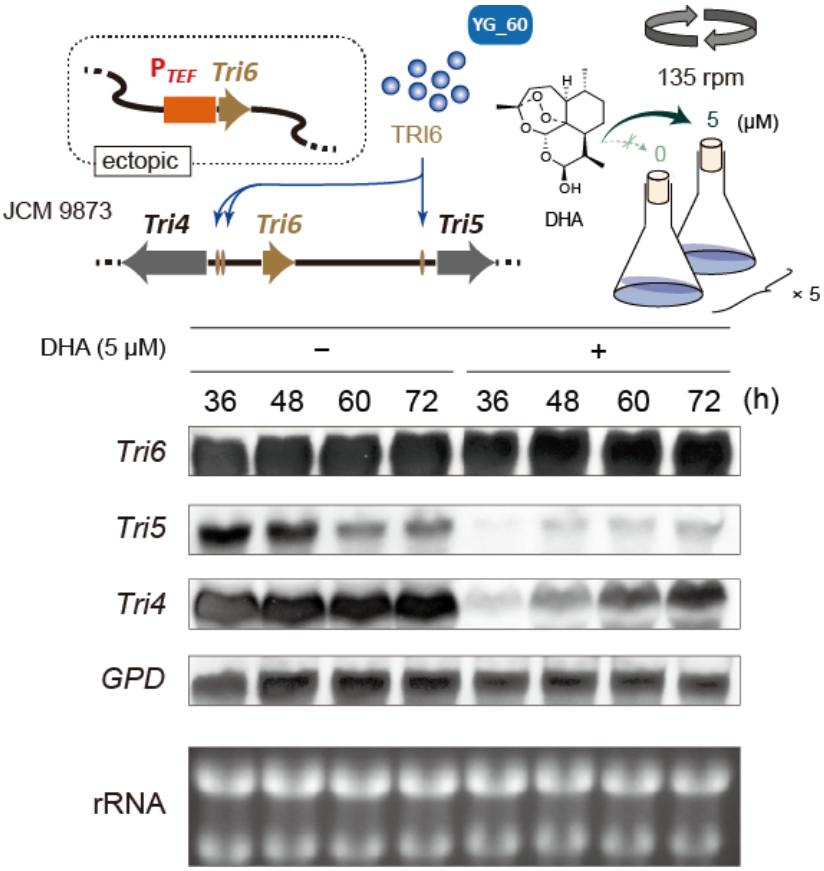

Figure 6. Northern blot analysis of RNA isolated from a constitutive *Tri6* overexpressor strain. The fungal strain was cultured in 30 mL YG_60 medium with or without 5 µM DHA in 100-mL Erlenmeyer flasks. The RNA blot (10 µg RNA each lane) was hybridized with DIG-labeled DNA probes for *Tri6*, *Tri5*, *Tri4*, and *GPD* (glyceraldehyde 3-phosphate dehydrogenase gene; FGSG_16627). The formaldehyde gel stained with ethidium bromide is shown below each lane to demonstrate equal RNA loading.

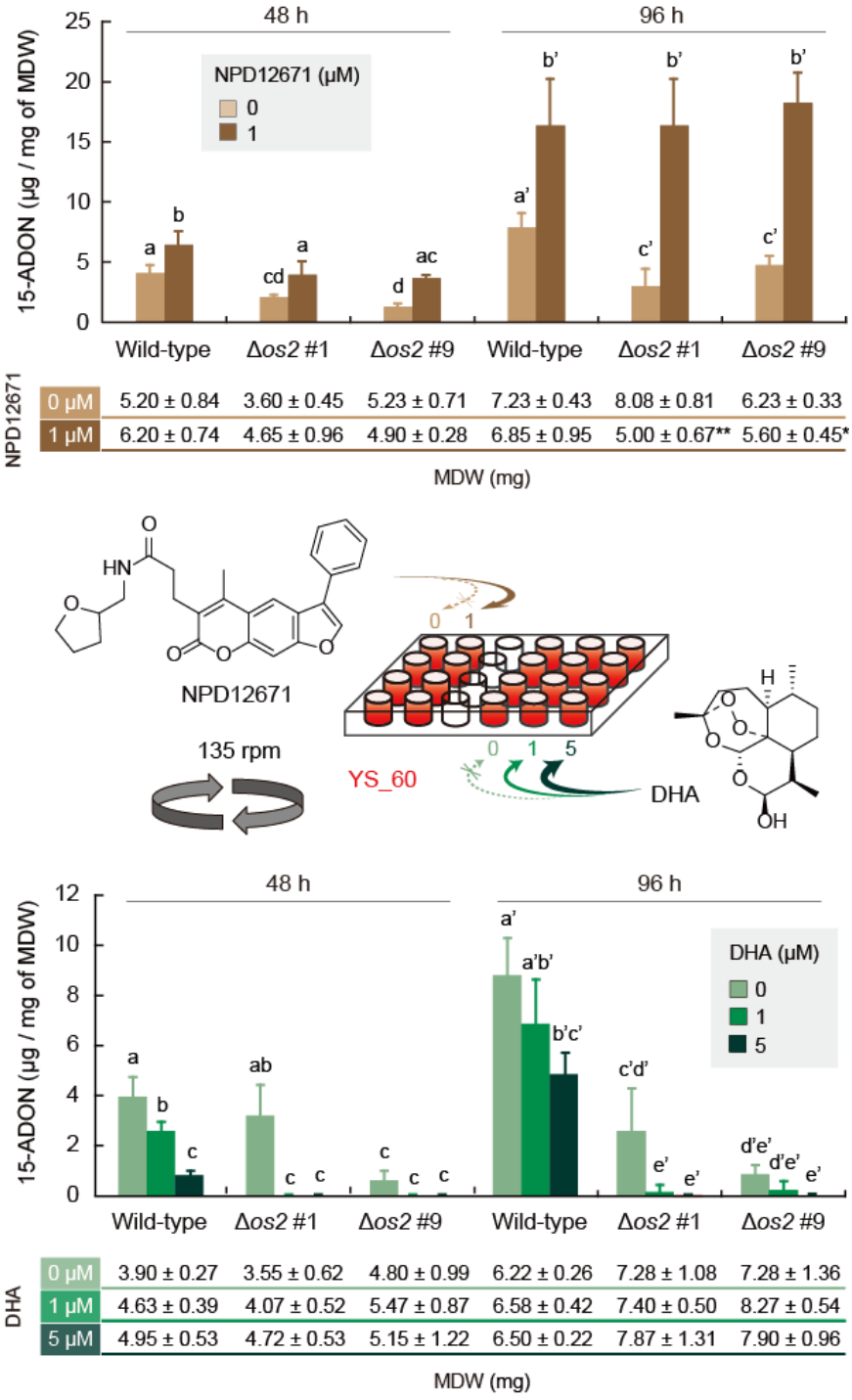

Figure 7. Effects of NPD12671 and DHA on 15-ADON production by wild-type and Δ*FgOs2* mutant strains grown under different culture conditions. Germinated spores (pre-culture) were inoculated into YS_60 medium and added to 24-well plates.

NPD12671 and DHA were added to the YS_60 culture at various concentrations as indicated. After 48 and 96 h of incubation, the amount of 15-ADON was quantified. Data were obtained from four independent pre-culture preparations. Different letters indicate significant differences analyzed by one-way ANOVA followed by Tukey-Kramer test ($P < 0.05$). Asterisks denote a significant difference (*$P < 0.05$, **$P < 0.01$; Student's *t* test) relative to untreated culture.

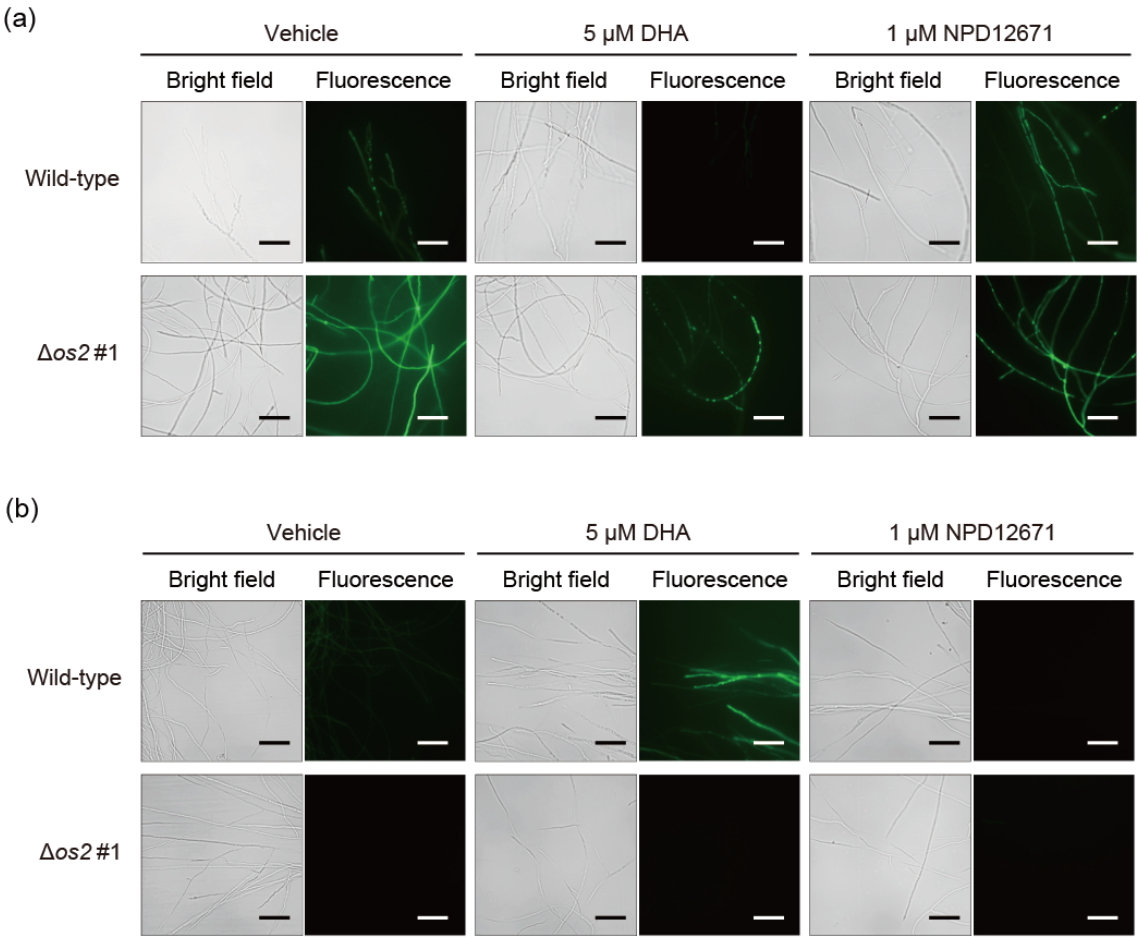

Figure 8. Epifluorescence microscopy of the WT and Δ*FgOs2* mutant treated with the H_2O_2-specific fluorescent dye BES-H_2O_2-Ac and the superoxide anion-specific fluorescent dye BES-So-AM. The young mycelia collected from YS_60 cultures (with carrier solvent DMSO, 5 μM DHA, and 1 μM NPD12671) in a 24-well plate (135 rpm and 25^{o}C for 16-24 h) were treated with 5 μM each of BES-H_2O_2-Ac (a) and BES-So-AM (b) for 1 h with gyratory shaking. After washing with water, the mycelia were observed under a BIOREVO BZ-9000 microscope (Keyence) with a GFP filter (excitation at 480/30 nm; emission at 510 nm, dichroic mirror wavelength, 505 nm). The scale bar on the image represents 50 μm.

Supporting Information

Identification and Characterization of Small Molecule Compounds That Modulate Trichothecene Production by *Fusarium graminearum*

Kazuyuki Maeda[†,‡], Hinayo Ichikawa[†], Yuichi Nakajima[†], Takayuki Motoyama[§], Shuichi Ohsato[‡], Kyoko Kanamaru[†], Tetsuo Kobayashi[†], Takumi Nishiuchi[∥], Hiroyuki Osada[§], Makoto Kimura[*,†]

[†] Graduate School of Bioagricultural Sciences, Nagoya University, Furo-cho, Chikusa-ku, Nagoya, Aichi 464-8601, Japan

[‡] Graduate School of Agriculture, Meiji University, 1-1-1 Higashi-Mita, Kawasaki, Kanagawa 214-8571, Japan

[§] Chemical Biology Research Group, RIKEN Center for Sustainable Resource Science, 2-1 Hirosawa, Wako, Saitama 351-0198, Japan

[∥] Advanced Science Research Centre, Kanazawa University, 13-1 Takaramachi, Kanazawa, Ishikawa 920-0934, Japan

Corresponding Author

*E-mail: mkimura@agr.nagoya-u.ac.jp

Background Information

Growth Inhibitory Activity of Artemisinins against Yeast and Malarial Parasites. Dihydroartemisinin (DHA), the first-generation analog of artemisinin, was developed by reducing its C-10 ketone for superior anti-malarial activity and bioavailability. In addition to their potent antimalarial activity, artemisinin analogs are known to show anticancer, antiviral, and wider antiparasitic properties.[1] Although artemisinins do not inhibit fungi growth, *Saccharomyces cerevisiae* is highly sensitive to these compounds on non-fermentable media, and to a lesser extent, on fermentable media.[2] Using yeast as a genetic model, subsequent studies revealed two distinct and competitive modes of action: a potent and specific mitochondria-dependent pathway and a less potent and less specific heme-mediated pathway.[3] Similar to yeast, malarial parasites in the *Plasmodium* genus are highly responsive to mitochondrial activation of artemisinin through reduction of the endoperoxide bridge in an electron transport chain-dependent manner, resulting in free radical generation and membrane potential depolarization.[1] In most types of cells including mammalian cells, however, such specific anti-mitochondrial actions do not occur. Instead, the latter relatively non-specific mode of actions proceed; heme-mediated cleavage of the endoperoxide causes generation of toxic free radicals and promiscuous binding of the activated artemisinin derivatives to numerous target proteins.[1] The differences in artemisinin sensitivity between organisms and cell types are explained by the available reducing agent level and free radical scavenging ability of the treated cells.

Supplementary Methods

Reagents. A chemical library of 456 chemicals dissolved at 10 mg mL^{-1} in dimethyl sulfoxide (DMSO) was provided from RIKEN Natural Products Depository (NPDepo). 5-methyl-3-phenyl-6-propyl-7*H*-furo(3,2-*g*)chromen-7-one (**1**) (Product Number R659142; discontinued as of 2017) was purchased from Sigma-Aldrich. DHA, artesunate (ATS), artemether (ATM), and artemisinin were obtained from Tokyo Chemical Industry. All chemicals were dissolved in DMSO (Biotechnology grade, Nacalai Tesque). HPLC-grade acetonitrile was obtained from Sigma-Aldrich; BES-H_2O_2-Ac, BES-So-AM, and other chemicals were purchased from Wako Pure Chemical Industries.

TLC Analysis. For semi-quantitative estimation of the amount of 15-ADON, TLC analysis was performed as described previously.[4] Briefly, the dried ethyl acetate extract was reconstituted in a small volume of ethanol, the metabolites were developed on a Kieselgel F_{254} TLC plate (Merck Millipore) using ethyl acetate/toluene (3:1), and trichothecenes were visualized with a color-developing reagent using 4-(*p*-nitrobenzyl)pyridine.

Quantification of Trichothecenes. To determine the effect of NPD12671 and artemisinin derivatives on 15-ADON production, an HPLC-UV method was used. The dried ethyl acetate-extract from each well of the 24-well plate culture was reconstituted in 120 µL of water/acetonitrile (75:25), and an aliquot (10 µL) was analyzed by a HPLC system (SCL-10A; Shimadzu) using a PEGASIL ODS SP100 column (diameter, 4.6 mm; length, 250 mm; Senshu Scientific). The column was run by isocratic elution with water/acetonitrile (75:25) at a flow rate of 1.0 mL min^{-1}. The total amount of 15-ADON (eluted at 9.5–9.7 min) was calculated from the peak area of the eluates monitored at 220 nm using a calibration curve obtained with 10–100 µg mL^{-1} of 15-ADON standard (standard mycotoxin mixture solution 2; Kanto Kagaku).

Nucleic Acid Manipulations. For RNA isolation, the collected mycelia were ground in liquid nitrogen in a mortar using the TriPure Isolation Reagent (Roche Diagnostics). DNA probes for northern blot analysis were prepared using a PCR DIG Probe synthesis kit (Roche Diagnostics) using primers listed in Table S2. Total RNA samples were separated on a 1.0% agarose gel containing formaldehyde (0.44 M), and then transferred to a Nytran® membrane (Schleicher & Schell) using a Turboblotter™ (Schleicher & Schell) blotting apparatus. Membranes were hybridized with digoxigenin (DIG)-labeled probes using DIG Easy Hyb (Roche Diagnostics) hybridization solution at 50°C, and washed as recommended by the manufacturer. Probe-RNA hybrid was detected by using a DIG Luminescent Detection kit (Roche Diagnostics).

Generation of Recombinant *Fusarium* Strains. To induce *Tri6* overexpression, pTef-Tri6-hph was constructed by inserting the coding region of *Tri6* between *Hin*dIII and *Spe*I sites of pAnTef-hph (Figure S6).[5] After linearization with *Xho*I, pTef-Tri6-hph was transformed into JCM 9873 and selected with 30 μg mL^{-1} hygromycin B.[6] A *Tri6* overexpressor strain, $Tri6^{O/E}$ #2s1, was established through conidium induction and subsequent single colony isolation of one high trichothecene-producing transformant. To disrupt *FgOs2*, pFgΔOs2-hph was created by placing a hygromycin B-resistant vector pCSN43 between the upstream and downstream regions of *FgOs2* (Figure S7). JCM 9873 was transformed with *Stu*I-linearized pFgΔOs2-hph and selected with hygromycin B (30 μg mL^{-1}). Two independent transformants, Δos2 #1 and #9, with targeted disruption of *FgOs2* were used for assaying trichothecene production.

Table S1. List of NPDepo Chemicals.

priority	plate	well No.	chemical	concentration	activation[a]	inhibition[b]	comments	experiments
highest	pilot-2	B04	NPD4346	2 μg mL^{-1}	+++	−	No growth inhibition. Increasing amount of 15-ADON detected at 5 and 10 μg mL^{-1}	triplicate
		F06	NPD4297	2 μg mL^{-1}	−	+++	No growth inhibition. Moderate inhibition of 15-ADON production at 1 μg mL^{-1}	triplicate
low	authentic	A07	indomethacin	1 μg mL^{-1}	+	−	No growth inhibition. No further increase in 15-ADON production at 10 μg mL^{-1}	duplicate
		B02	cycloheximide	1 μg mL^{-1}	−	−	Moderate inhibition of 15-ADON production at 10 μg mL^{-1} with growth inhibition	duplicate
		B03	$C_{36}H_{62}O_{11}$ [c]	2 μg mL^{-1}	−	++	Abnormal growth	triplicate
		B10	G-418	1 μg mL^{-1}	−	+++	Strong growth inhibition	triplicate
		C06	neomycin B	1 μg mL^{-1}	−	−	Strong inhibition of 15-ADON production at 10 μg mL^{-1} with growth inhibition	duplicate
		D03	camptothecin	1 μg mL^{-1}	−	++	Strong growth inhibition	duplicate
		D07	nocodazole	1 μg mL^{-1}	−	−	Weak inhibition of 15-ADON production at 10 μg mL^{-1} without growth inhibition	duplicate
		D11	colistin A	1 μg mL^{-1}	−	−	Strong inhibition of 15-ADON production at 10 μg mL^{-1} with growth inhibition	duplicate
		E05	benomyl	1 μg mL^{-1}	−	−	Strong inhibition of 15-ADON production at 10 μg mL^{-1} with growth inhibition	duplicate
		E09	griseofulvin	2 μg mL^{-1}	−	−	Strong inhibition of 15-ADON production at 10 μg mL^{-1} with growth inhibition	duplicate
		E10	$C_8H_{10}N_2O_4$ [d]	2 μg mL^{-1}	−	−	Inhibition of 15-ADON production at 10 μg mL^{-1} in one experiment	duplicate
		F05	perphenazine	1 μg mL^{-1}	−	−	Moderate inhibition of 15-ADON production at 10 μg mL^{-1} with growth inhibition	duplicate
		G04	$C_{26}H_{28}Cl_2F_2N_2$ [e]	1 μg mL^{-1}	−	−	Strong inhibition of 15-ADON production at 10 μg mL^{-1} with growth inhibition	duplicate
		G05	gemfibrozil	1 μg mL^{-1}	−	−	Weak activation of 15-ADON production at 10 μg mL^{-1} without growth inhibition	duplicate
		G11	tolnaftate	1 μg mL^{-1}	−	++	Moderate growth inhibition	duplicate
		H02	$C_{25}H_{30}ClI_2NO_3$ [f]	1 μg mL^{-1}	−	−	Strong inhibition of 15-ADON production at 10 μg mL^{-1} with growth inhibition	duplicate
		H05	niclosamide	1 μg mL^{-1}	−	−	Strong inhibition of 15-ADON production at 10 μg mL^{-1} with growth inhibition	duplicate
		H07	siccanin	1 μg mL^{-1}	−	−	Strong inhibition of 15-ADON production at 10 μg mL^{-1} with growth inhibition	duplicate
		H09	reveromycin A	1 μg mL^{-1}	−	++	Moderate growth inhibition	duplicate
		H10	staurosporine	1 μg mL^{-1}	−	++	Moderate growth inhibition	duplicate
	pilot-1	A03	undisclosed	1 μg mL^{-1}	−	−	Strong inhibition of 15-ADON production at 10 μg mL^{-1} with growth inhibition	duplicate
		C05	undisclosed	1 μg mL^{-1}	−	−	Weak activation of 15-ADON production at 10 μg mL^{-1} without growth inhibition	duplicate
		C09	undisclosed	1 μg mL^{-1}	−	−	Weak inhibition of 15-ADON production at 10 μg mL^{-1} with small inhibition	duplicate
		D06	undisclosed	2 μg mL^{-1}	−	++	Moderate growth inhibition	triplicate
		E04	undisclosed	1 μg mL^{-1}	−	−	Weak activation of 15-ADON production at 10 μg mL^{-1} without growth inhibition	duplicate
		E08	undisclosed	1 μg mL^{-1}	−	−	Weak activation of 15-ADON production at 10 μg mL^{-1} without growth inhibition	duplicate
		H02	undisclosed	1 μg mL^{-1}	−	−	Strong inhibition of 15-ADON production at 10 μg mL^{-1} with growth inhibition	duplicate
		H07	$C_{25}H_{30}N_2O_5$ [g]	2 μg mL^{-1}	−	−	Weak inhibition of 15-ADON production at 5 μg mL^{-1} without growth inhibition	triplicate

pilot-2	A10	undisclosed	2 μg mL^{-1}	−	−	Weak activation of 15-ADON production at 10 μg mL^{-1} without growth inhibition	triplicate
	C02	undisclosed	1 μg mL^{-1}	−	−	Weak activation of 15-ADON production at 10 μg mL^{-1} without growth inhibition	duplicate
	C05	undisclosed	1 μg mL^{-1}	−	−	Weak activation of 15-ADON production at 10 μg mL^{-1} without growth inhibition	duplicate
	C11	undisclosed	1 μg mL^{-1}	−	−	Weak activation of 15-ADON production at 10 μg mL^{-1} without growth inhibition	duplicate
	D07	undisclosed	1 μg mL^{-1}	−	−	Weak activation of 15-ADON production at 10 μg mL^{-1} without growth inhibition	duplicate
	D11	undisclosed	2 μg mL^{-1}	−	−	Strong inhibition of 15-ADON production at 10 μg mL^{-1} with small growth inhibition	duplicate
	E05	undisclosed	1 μg mL^{-1}	−	−	Weak activation of 15-ADON production at 10 μg mL^{-1} without growth inhibition	duplicate
	E07	undisclosed	1 μg mL^{-1}	−	−	Weak activation of 15-ADON production at 10 μg mL^{-1} without growth inhibition	duplicate
	E08	undisclosed	1 μg mL^{-1}	−	−	Weak activation of 15-ADON production at 10 μg mL^{-1} without growth inhibition	duplicate
	F05	undisclosed	2 μg mL^{-1}	−	−	Moderate inhibition of 15-ADON production at 10 μg mL^{-1} without growth inhibition	duplicate
	F10	undisclosed	1 μg mL^{-1}	−	−	Strong inhibition of 15-ADON production at 10 μg mL^{-1} with growth inhibition	duplicate
	G04	undisclosed	2 μg mL^{-1}	−	−	Moderate inhibition of 15-ADON production at 10 μg mL^{-1} without growth inhibition	duplicate
	G09	undisclosed	1 μg mL^{-1}	−	−	Weak activation of 15-ADON production at 10 μg mL^{-1} without growth inhibition	duplicate
	H08	undisclosed	1 μg mL^{-1}	−	−	Weak activation of 15-ADON production at 10 μg mL^{-1} without growth inhibition	duplicate
pilot-3	A09	undisclosed	1 μg mL^{-1}	−	−	Weak inhibition of 15-ADON production at 10 μg mL^{-1} without growth inhibition	duplicate
	B04	undisclosed	1 μg mL^{-1}	−	−	Strong inhibition of 15-ADON production at 10 μg mL^{-1} with growth inhibition	duplicate
	B06	undisclosed	1 μg mL^{-1}	+	−	No growth inhibition	duplicate
	B09	undisclosed	1 μg mL^{-1}	−	−	Moderate inhibition of 15-ADON production at 10 μg mL^{-1} without growth inhibition	duplicate
	C03	$C_{16}H_{15}N_5$ [h]	1 μg mL^{-1}	−	+++	Strong growth inhibition	duplicate
	C06	undisclosed	1 μg mL^{-1}	−	−	Weak activation of 15-ADON production at 10 μg mL^{-1} without growth inhibition	duplicate
	C07	$C_{53}H_{102}N_{16}O_{17}S$ [i]	1 μg mL^{-1}	−	+++	Moderate growth inhibition	duplicate
	D06	undisclosed	1 μg mL^{-1}	−	−	Moderate inhibition of 15-ADON production at 10 μg mL^{-1} without growth inhibition	duplicate
	E03	undisclosed	1 μg mL^{-1}	−	−	Weak activation of 15-ADON production at 10 μg mL^{-1} without growth inhibition	duplicate
	F05	undisclosed	1 μg mL^{-1}	−	−	Moderate inhibition of 15-ADON production at 10 μg mL^{-1} without growth inhibition	duplicate
	H02	undisclosed	1 μg mL^{-1}	−	+	No growth inhibition	duplicate
	H06	undisclosed	1 μg mL^{-1}	−	+	No growth inhibition	duplicate
pilot-4	A09	undisclosed	1 μg mL^{-1}	−	−	Weak activation of 15-ADON production at 10 μg mL^{-1} without growth inhibition	duplicate
	B04	undisclosed	1 μg mL^{-1}	−	−	Weak activation of 15-ADON production at 10 μg mL^{-1} without growth inhibition	duplicate
	C04	undisclosed	1 μg mL^{-1}	−	−	Weak inhibition of 15-ADON production at 10 μg mL^{-1} with small inhibition	duplicate
	F07	$C_{26}H_{29}NO_2$ [j]	1 μg mL^{-1}	−	−	Weak inhibition of 15-ADON production at 10 μg mL^{-1} with small inhibition	duplicate
	G04	undisclosed	1 μg mL^{-1}	−	−	Weak activation of 15-ADON production at 10 μg mL^{-1} without growth inhibition	duplicate
	H09	undisclosed	1 μg mL^{-1}	−	−	Strong inhibition of 15-ADON production at 10 μg mL^{-1} with growth inhibition	duplicate
pilot-5	A09	undisclosed	2 μg mL^{-1}	−	−	Moderate inhibition of 15-ADON production at 5 μg mL^{-1} with small growth inhibition	duplicate
	B04	undisclosed	2 μg mL^{-1}	−	−	Strong inhibition of 15-ADON production at 10 μg mL^{-1} with small growth inhibition	duplicate
	B08	undisclosed	2 μg mL^{-1}	−	−	Weak activation of 15-ADON production at 10 μg mL^{-1} without growth inhibition	duplicate

B10	undisclosed	2 μg mL^{-1}	−	−	Moderate activation of 15-ADON production at 10 μg mL^{-1} without growth inhibition	duplicate
B11	undisclosed	2 μg mL^{-1}	−	−	Strong inhibition of 15-ADON production at 10 μg mL^{-1} with growth inhibition	duplicate
D03	undisclosed	2 μg mL^{-1}	−	−	Weak inhibition of 15-ADON production at 10 μg mL^{-1} without growth inhibition	duplicate
E02	$C_{21}H_{24}N_2O_3S$ [k]	2 μg mL^{-1}	+	+	No growth inhibition. Activation or inhibition depending on pre-culture conditions	triplicate
E11	$C_{27}H_{29}N_3OS$ [l]	2 μg mL^{-1}	−	−	Strong inhibition of 15-ADON production at 10 μg mL^{-1} with small growth inhibition	triplicate
F02	$C_{17}H_{19}NO_3S$ [m]	2 μg mL^{-1}	−	+	No growth inhibition	duplicate
F03	$C_{24}H_{22}ClN_5OS$ [n]	2 μg mL^{-1}	−	−	Strong inhibition of 15-ADON production at 10 μg mL^{-1} with growth inhibition	duplicate
F06	undisclosed	2 μg mL^{-1}	−	−	Moderate inhibition of 15-ADON production at 10 μg mL^{-1} without growth inhibition	duplicate

The hit chemicals listed in this table modulated trichothecene production when added to the 24-well plate culture at 10 μg mL^{-1}.

[a]The relative trichothecene induction activity of each chemical in YS_60 medium is shown by plus and minus signs; +++, strong activation; ++, moderate activation; +, weak activation; −, no activation.

[b]The relative trichothecene inhibition activity of each chemical in YS_60 medium is shown by plus and minus signs; +++, strong inhibition; ++, moderate inhibition; +, weak inhibition; −, no inhibition.

[c]monensin sodium salt

[d]L-mimosine from Koa hoale seeds

[e]flunarizine hydrochloride

[f]amiodarone hydrochloride

[g]2-(4,11-dimethyl-2-oxo-6,7,8,9-tetrahydro-[1]benzofuro[3,2-*g*]chromen-3-yl)-*N*-(2-morpholin-4-ylethyl)acetamide (NPD5026)

[h]4',6-diamidino-2-phenylindole dehydrochloride (DAPI)

[i]colistin sulfate salt

[j]3-(2-hydroxy-3,4-dimethylphenyl)-3-phenyl-*N*-(1-phenylpropan-2-yl)propenamide (NPD115)

[k]3-({[4-(2,5-dimethylphenyl)-5-methyl-1,3-thiazol-2-yl]amino}carbonyl)bicyclo[2.2.1]heptane-2-carboxylic acid

[l]6-(4-ethoxy-phenyl)-4-phenyl-2-(2-piperidin-1-yl-ethylsulfanyl)-nicotinonitrile

[m]ethyl 2-(butanoylamino)-4-phenylthiophene-3-carboxylate

[n]8-(4-chloro-phenyl)-5-(3-dimethylamino-propyl amino)-10-thia-6,6*a*,11-triaza-cyclopenta-[*b*]phenanthren-7-one

Table S2. Primers Used for PCR.

primer	sequence (5'-3')	description[a]
#01: Tri6-probe-Fw	GCCGAATCTCACTACGAATCT	Primer for preparation of *Tri6* probe and the probe I
#02: Tri6-probe-Rev	AGTGATCTCGCATGTTATCCA	Primer for preparation of *Tri6* probe and the probe I
#03: Tri5-probe-Fw	TTTCTCAACACTAGCGTGCGC	Primer for preparation of *Tri5* probe
#04: Tri5-probe-Rev	GCAGAACTTCTTGGCGTCCTC	Primer for preparation of *Tri5* probe
#05: Tri4-probe-Fw	CGAGAGAATACTGGCCGTCCT	Primer for preparation of *Tri4* probe
#06: Tri4-probe-Rev	GAGATCTCCAAGATGCACGAT	Primer for preparation of *Tri4* probe
#07: FPPS-probe-Fw	GAAGTCTCTCGAGGCCAACCC	Primer for preparation of *FPPS* probe
#08: FPPS-probe-Rev	GCCACCGCTCTCGTCAATGT	Primer for preparation of *FPPS* probe
#09: Gpd-probe-Fw	GGTCGTATCGGCCGTATCGTCTTC	Primer for preparation of *GPD* probe
#10: Gpd-probe-Rev	TGGGTGGCAGTGTAGGAGTGGA	Primer for preparation of *GPD* probe
#11: hph-PR1	GGGGCGTCGGTTTCCACTATCG	Primer for preparation of the probe II
#12: hph-PL1	AGCTGCGCCGATGGTTTCTACAA	Primer for preparation of the probe II
#13: JCMTri6-HindIII_S	TCTAAGCTTATGATTTACATGGAGGCCGAATCT	Primer for construction of pTef-Tri6-hph (*Hin*dIII site created for vector cloning)
#14: FL-jTri6_SpeI_AS	CATACTAGTCAACACTTATGTATCCGCCT	Primer for construction of pTef-Tri6-hph (*Spe*I site created for vector cloning)
#15: dFgOs2_1F_StuI	TTAGGCCTAACGTTCGGCAAGGGGATGAA	Inward primer for construction of pFgΔOs2-hph (*Stu*I site created for IPCR)
#16: dFgOs2_2R_StuI	TTAGGCCTCGACCCAACAGGAAGCAATCC	Inward primer for construction of pFgΔOs2-hph (*Stu*I site created for IPCR)
#17: dFgOs2_3F_HindIII	TTAAGCTTAGCTGCAGAACGAGGAACAGG	Outward primer for construction of pFgΔOs2-hph (*Hin*dIII site created for vector cloning)
#18: dFgOs2_4R_SmaI	AACCCGGGGCCCATGATCTATCCCACCAC	Outward primer for construction of pFgΔOs2-hph (*Sma*I site created for vector cloning)
#19: dFgOs2_Long_F	AGCGACAAGTGTTGACCCTCG	Primer for screening of *FgOs2* disruptant
#20: dFgOs2_Long_R	TGCCCTCCCATCCCTTATGTT	Primer for screening of *FgOs2* disruptant
#21: check on trpC	TGAATGCTCCGTAACACCCAATA	Primer for screening of the *FgOs2* and *FgNde1* disruptants
#22: check on SacI side	CACTAAAGGGAACAAAAGCTG	Primer for screening of the *FgOs2* and *FgNde1* disruptants
#23: FgOs2-probe-F	TTCGTGGTATCATCGGCACTG	Primer for preparation of the probe III
#24: FgOs2-probe-R	GTTTGTACGCGCCCAGATCTT	Primer for preparation of the probe III
#25: dFgNde1_1F_HpaI	AAGTTAACAACTTAGAAGCTCCGCATGTT	Inward primer for construction of pFgΔNde1-hph (*Hpa*I site created for IPCR)
#26: dFgNde1_2R_HpaI	AAGTTAACAAATCGCGCATGTTTAGTAAC	Inward primer for construction of pFgΔNde1-hph (*Hpa*I site created for IPCR)
#27: dFgNde1_3F_SmaI	AACCCGGGAGCAAGTAGTGTTCGGTTTGT	Outward primer for construction of pFgΔNde1-hph (*Sma*I site created for vector cloning)
#28: dFgNde1_4R_NotI	ATAAGCGGCCGCACGCCTGGTACAGATATGCTA	Outward primer for construction of pFgΔNde1-hph (*Not*I site created for vector cloning)
#29: dFgNde1_Long_F	TCGGCTTTGGATGGGATATTG	Primer for screening of *FgNde1* disruptant
#30: dFgNde1_Long_R	GATGCAGGGCGAGGTAAGCTA	Primer for screening of *FgNde1* disruptant

#31: FgNde1-probe-F	CGCCATGAGACTGAACAATAC	Primer for preparation of the probe IV
#32: FgNde1-probe-R	TGGCATTCTCAGCACCGACAC	Primer for preparation of the probe IV
#33: Pks12-F	GGAGAAATGATTGCGATACAG	Primer for preparation of *PKS12* probe
#34: Pks12-R	CTACAAGCTCCTTGAGATTGG	Primer for preparation of *PKS12* probe

[a]Restriction enzyme recognition sites created in primers are underlined.

		R_1	R_2	R_3	activation
hit chemical	NPD4346	—H	H	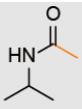	+
analogs	NPD4893	—CH_3	H	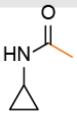	– 5 µg/ml in YS_60
	NPD9811	—H	CH_3	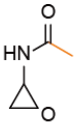	+
	NPD3387	—H	CH_3	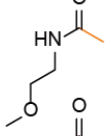	+++
	NPD3486	—H	CH_3	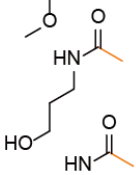	++
	NPD4916	—H	H	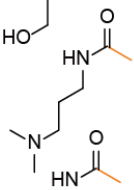	– 5 µg/ml in YS_60
	NPD4748	—H	H	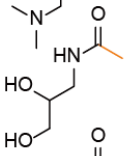	–
	NPD3295	—H	H	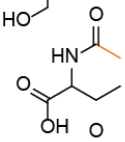	++
	NPD12671	—H	H	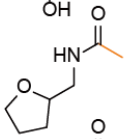	+++
	NPD4434	—H	H	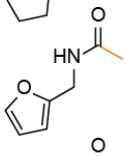	++
	NPD12918	—H	H	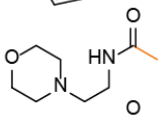	–
	NPD9801	—H	H	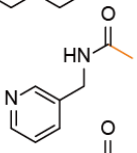	+
	NPD12239	—H	H	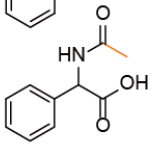	+
	1	—H	H		– 5 µg/ml in YS_60

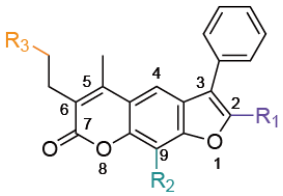

1: 5-methyl-3-phenyl-6-propyl-7*H*-furo(3,2-*g*)chromen-7-one

Figure S1. NPD4346 and its analogs tested for their ability to stimulate trichothecene biosynthesis. For the trichothecene production assay, *F. graminearum* JCM 9873 was inoculated into YG_60 medium, added to the wells in a 24-well plate, and treated with 10 μg mL^{-1} of each chemical, unless otherwise noted. These chemicals differ in the three functional groups ($-R_1$, $-R_2$, $-C_2H_4-R_3$) attached to the linear furanocoumarin (psoralen) skeleton. The amount of 15-ADON was evaluated by TLC of the ethyl acetate extract of the culture at 48 h (Figure S2). The relative trichothecene induction activity of each chemical is shown by plus and minus signs; +++, strong activation; ++, moderate activation; +, weak activation; −, no activation.

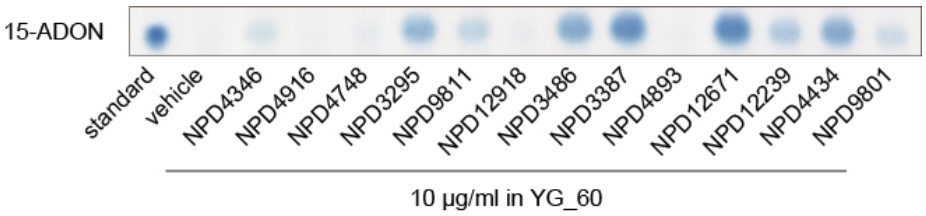

Figure S2. Trichothecene production by *F. graminearum* JCM 9873 cultured in the presence of 10 μg mL^{-1} NPDepo chemicals. Each lane of TLC contains ethyl acetate extract from 0.6 mL of YG_60 culture. 15-ADON was separated and visualized as previously described.[4]

		inhibition	R
hit chemical	NPD4297	++	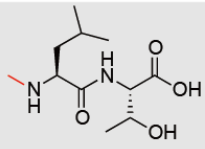
analogs	NPD4166	++	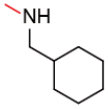
	NPD4234	+++	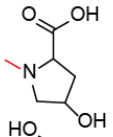
	NPD4365	+	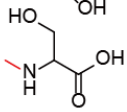
	NPD3475	– 5 µg/ml	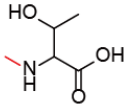
	NPD3013	– 5 µg/ml	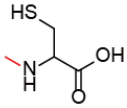
	NPD2604	+++	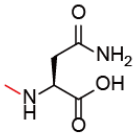
	NPD7699	+++	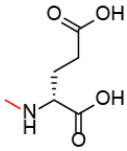
	NPD13541	++	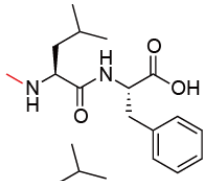
	NPD13543	++	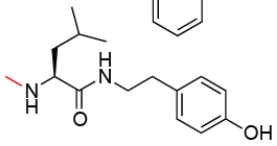
	NPD3902	+++	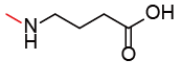
	NPD4037	++	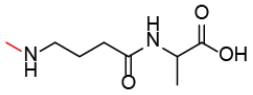
	NP28	+++	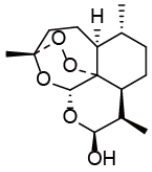

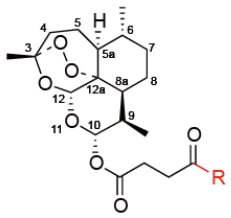

Figure S3. NPD4297 and its analogs tested for their ability to inhibit trichothecene biosynthesis. Except for NP28, these chemicals differ in the functional group (R) amide-bonded to the hemisuccinate linker of ATS. To evaluate these compounds' relative inhibitory activity against trichothecene production, *F. graminearum* JCM 9873 was grown in YS_60 medium containing 1 μg mL^{-1} of each chemical for 48 h in a 24-well plate. For NPD3475 and NPD3013, their concentrations in the medium were increased to 5 μg mL^{-1}. After extracting the culture with ethyl acetate, the amount of 15-ADON was evaluated using TLC. The relative trichothecene inhibition activity of each chemical is shown by plus and minus signs; +++, strong inhibition; ++, moderate inhibition; +, weak inhibition; −, no inhibition.

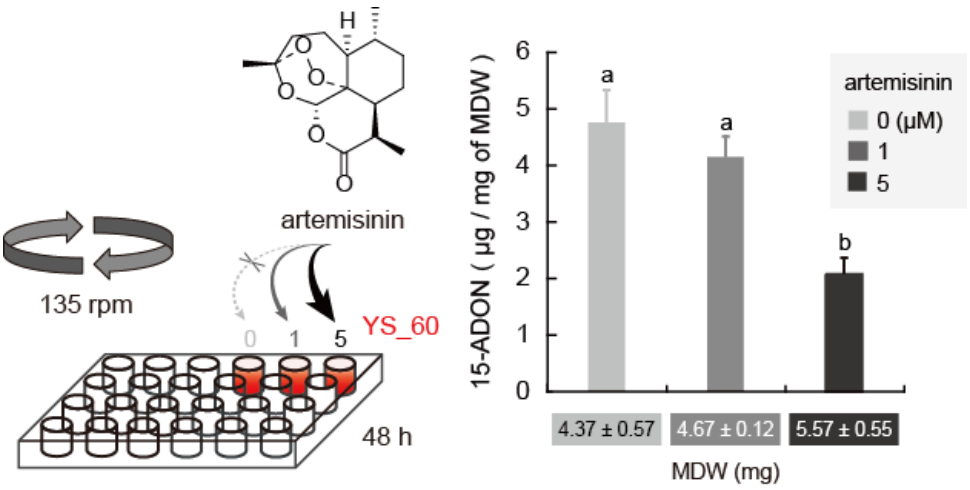

Figure S4. Inhibitory activity of artemisinin on trichothecene production by *F. graminearum* JCM 9873. The inhibitory activity was determined by the 24-well plate culture method as described for artemisinin derivatives (Figure 4). Data were obtained from triplicate experiments, each using an independent pre-culture. Different letters

indicate significant differences analyzed by one-way ANOVA followed by Tukey-Kramer test ($P < 0.01$).

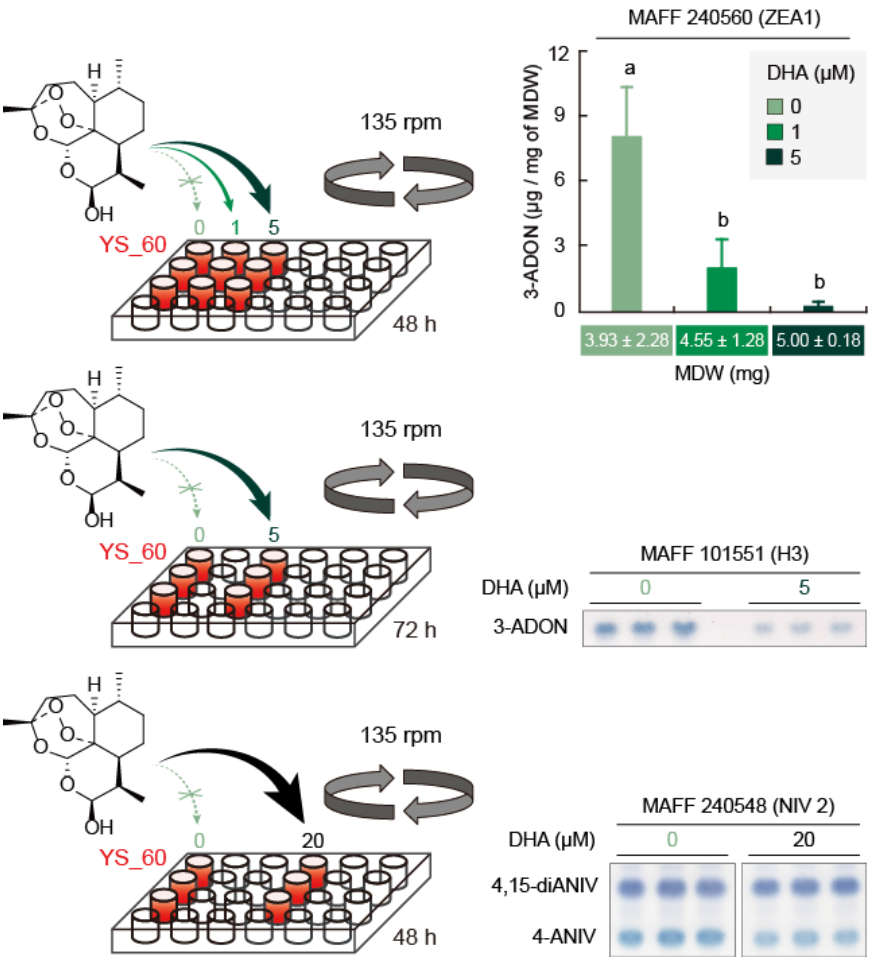

Figure S5. Inhibitory activity of DHA on trichothecene production by various strains of *F. graminearum*. The fungal cultures were incubated for the designated periods. Data were obtained from triplicate experiments. For strains MAFF 101551 and MAFF 240548, the amount of trichothecenes was estimated by TLC analysis. For strain MAFF 240560, 3-ADON was quantified by HPLC; different letters indicate significant differences analyzed by one-way ANOVA followed by Tukey-Kramer test ($P < 0.01$).

The effects of inhibition were obviously different among strains under the assay conditions.

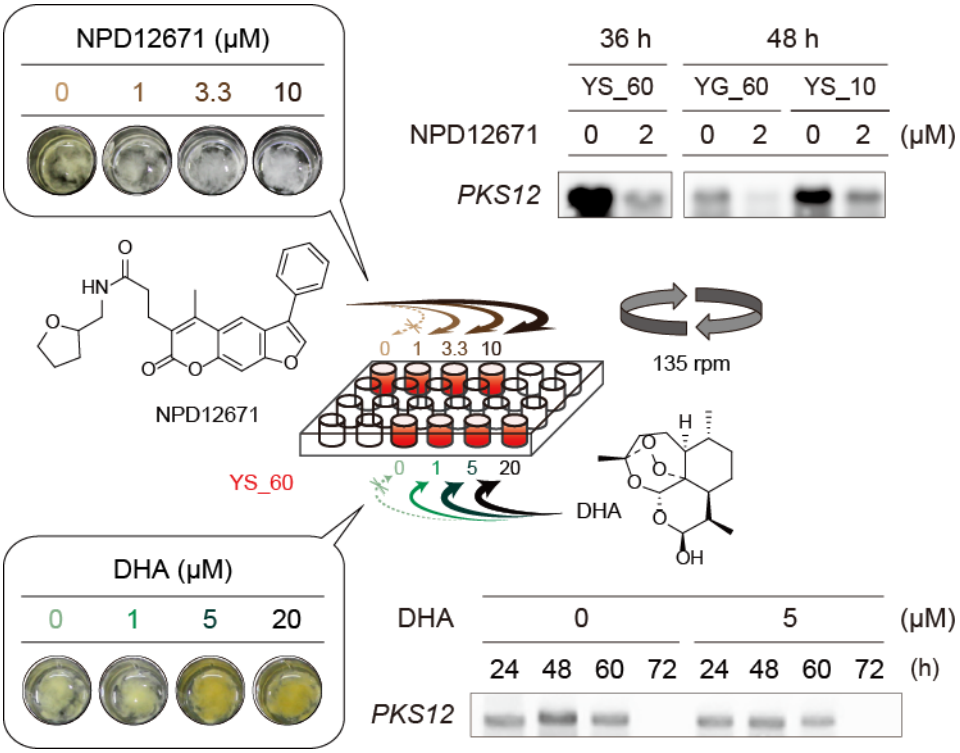

Figure S6. Effects of NPD12671 and DHA on mycelial pigmentation. Typical pigmentation patterns of *F. graminearum* JCM 9873 cultured in the presence of NPD12671 and DHA were photographed (left panels). To see whether the differences in pigmentation patterns are associated with aurofusarin biosynthesis, expression of *PKS12* was analyzed. The same RNA samples used for investigations of *Tri* gene expression in the NPD12671 and DHA-treated cultures (Figure 3 and Figure 5, respectively) were used for northern blot analyses (see Table S2 for primers used for preparation of the *PKS12* probe).

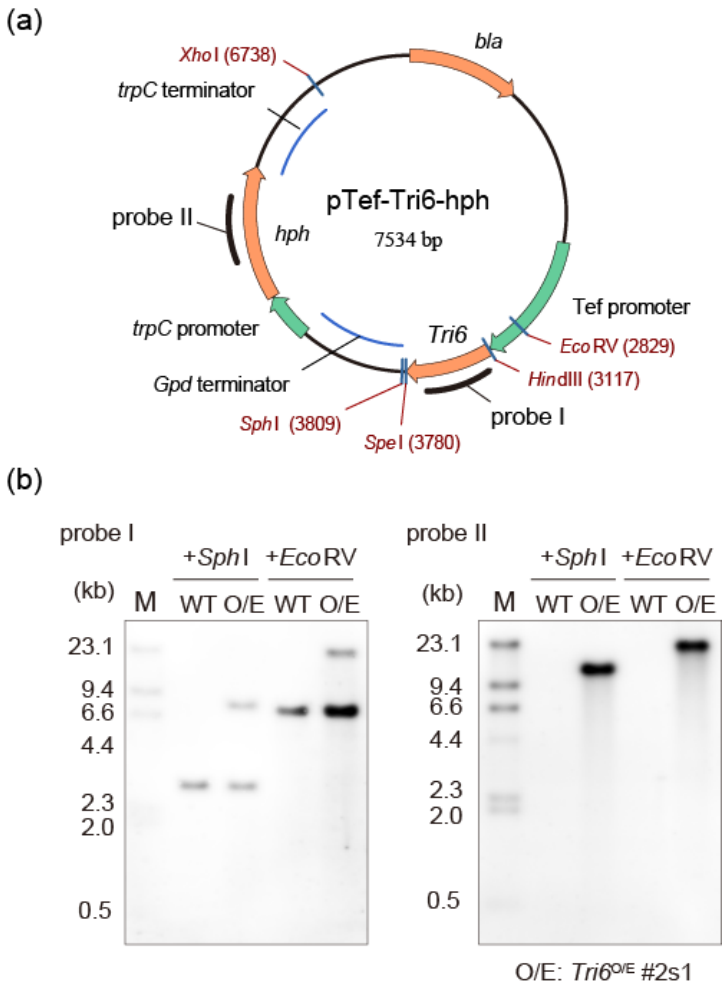

Figure S7. Overexpression of *Tri6* in *F. graminearum*. (a) Structure of the *Tri6* overexpression vector, pTef-Tri6-hph. The vector contains the hygromycin phosphotransferase gene (*hph*) for selection with hygromycin B. After linearization with *Xho*I, the vector was transformed into JCM 9873 and selected with 30 μg mL^{-1} hygromycin B as previously described.[7] (b) Analysis of the integration pattern of the *Tri6* expression cassette in the genome of strain $Tri6^{O/E}$ #2s1. Genomic DNA of the wild-type (WT) and *Tri6* overexpressor strains were digested with *Sph*I and *Eco*RV, and hybridized with probes I (*Tri6*) and II (*hph*), respectively. Probes were synthesized with a PCR DIG probe synthesis kit using primers listed in Table S2.

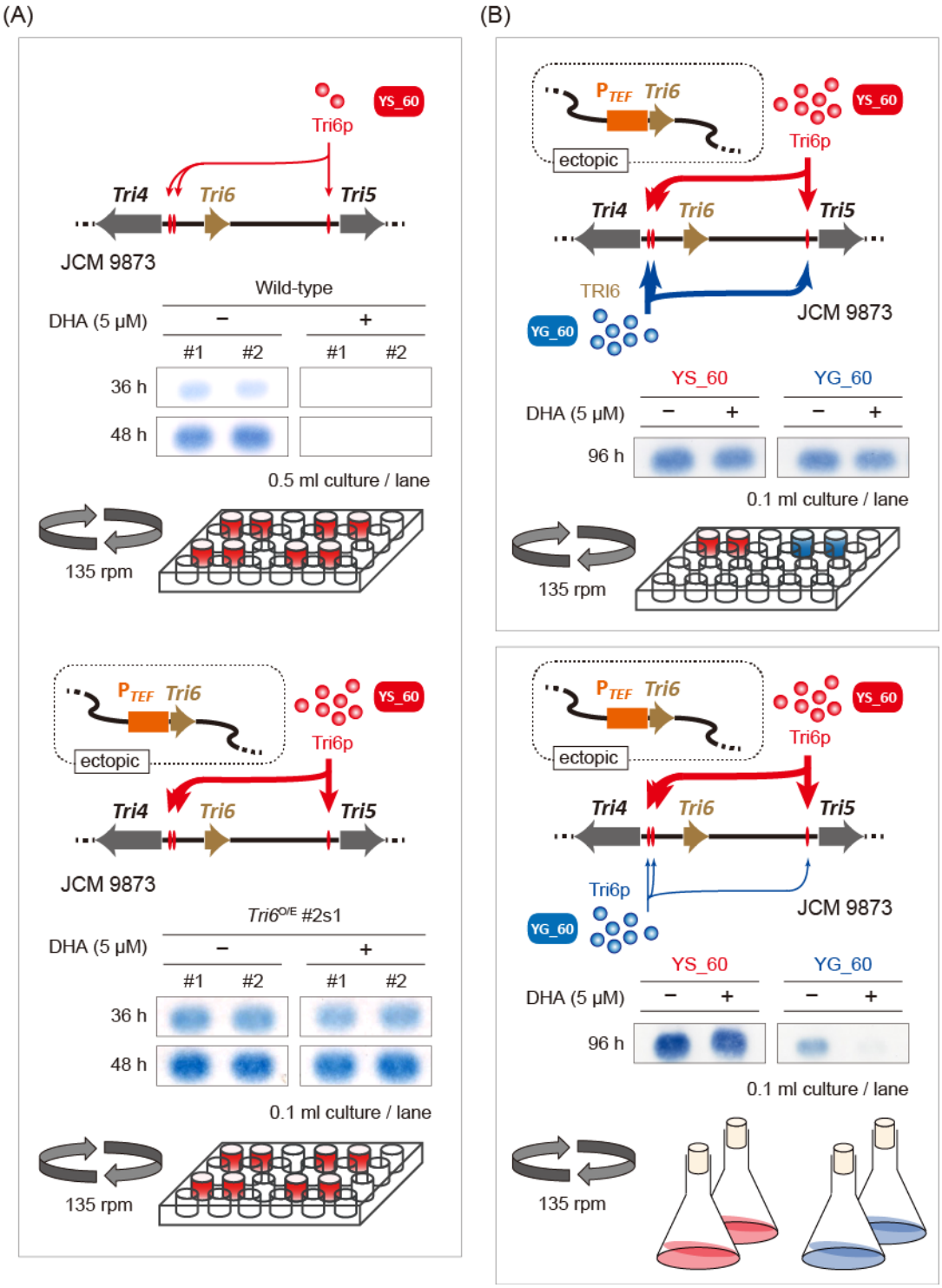

Figure S8. Effect of DHA on 15-ADON production by wild-type and constitutive *Tri6* overexpressor (*Tri6*$^{O/E}$ #2s1) strains grown under different culture conditions. (a)

Pre-cultures of wild-type and constitutive *Tri6* overexpressor strains were inoculated to YS_60 medium with or without 5 μM DHA and 1-mL aliquots were distributed into 24-well plates. After incubating for 36 and 48 h, the metabolites were extracted with ethyl acetate and analyzed by TLC. A blue spot of 15-ADON was visualized by the color reaction. Each lane contains metabolites from 0.5 (wild-type) and 0.1 mL (overexpressor) of culture. The experiment was performed in duplicate (#1 and #2) using independent preparations of pre-cultures. (b) Pre-culture of the constitutive *Tri6* overexpressor strain was inoculated into YS_60 and YG_60 media with or without 5 μM DHA. The cultures were added to a 24-well plate (upper panel; 1-mL scale culture) or 100-mL Erlenmeyer flasks (lower panel; 30-mL scale culture), and incubated with gyratory shaking for 96 h. The ethyl acetate extract of 0.1 mL culture was applied to each TLC lane. Although the amount of 15-ADON that accumulated in the YG_60 culture in Erlenmeyer flasks differed considerably depending on the yeast extract lots, pre-culture preparations, and media used for the assay (*i.e*., time the autoclaved media were taken out of the chamber after 15 min of sterilization), we optimized conditions under which DHA inhibited trichothecene production in the *Tri6* overexpressor. Red vertical discs represent Tri6p-binding sites. Red and blue circles are Tri6p produced by culturing the fungus in YS_60 and YG_60 media, respectively.

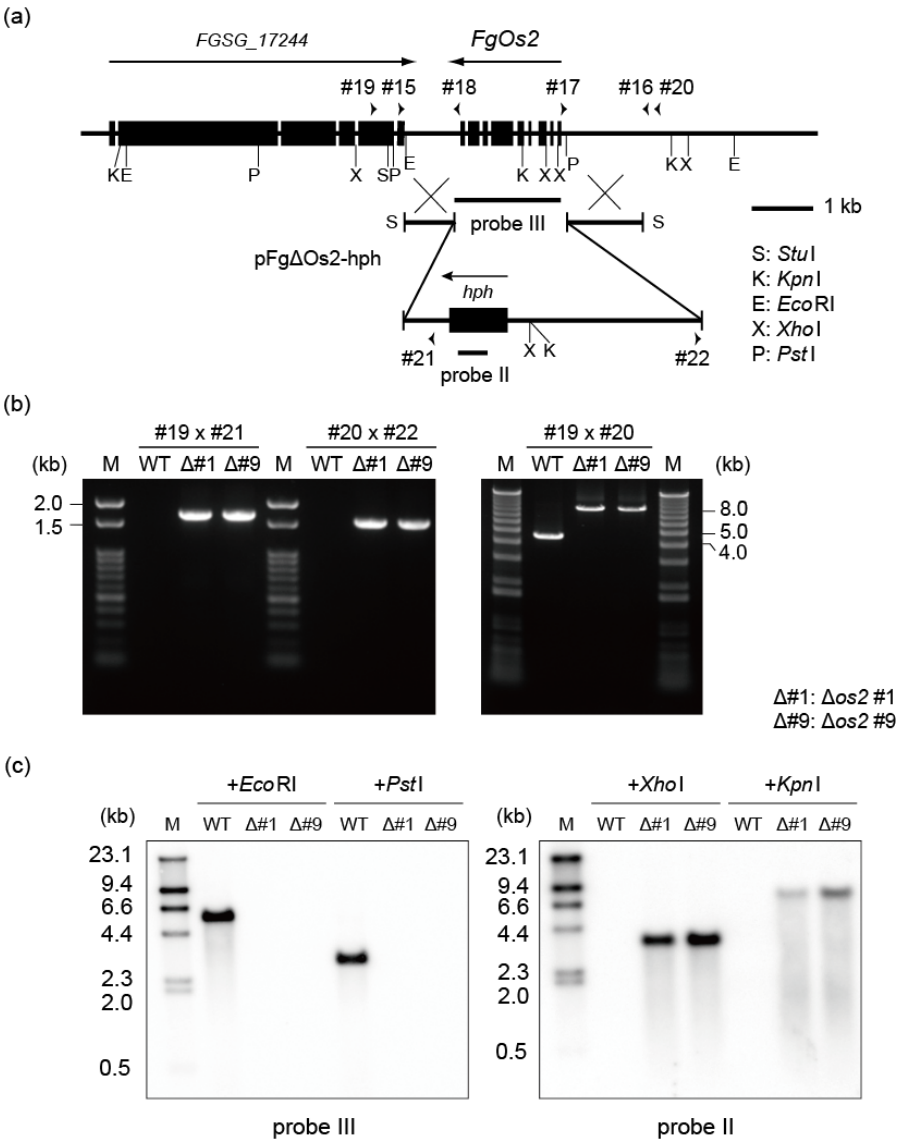

Figure S9. Disruption of *FgOs2* in *F. graminearum* JCM 9873. (a) Strategy of the *FgOs2* gene (FGSG_09612) disruption. *FgOs2* disruption vector pFgΔOs2-hph was constructed by replacing the whole coding region with pCSN43 that contains the *hph* cassette by the inverse PCR (IPCR) method[8] (see Table S2 for primer sequences). (b) PCR confirmation of gene disruption. PCR was performed with primers that specifically amplify the junction between the *FgOs2* gene-flanking region and gene disruption vector (#19 × #21 and #20 × #22) and primers that amplify across the deleted region (#19 × #20). Expected bands characteristic of the *FgOs2* deletion (mutant strains Δ*os*2

#1 and #9) were amplified with primers #19 and #21 (1.5 kb), #20 and #22 (1.4 kb), and #19 and #20 (8.1 kb); an expected amplicon size of 4.5 kb was obtained from the wild-type (WT) genome with primers #19 and #20. (c) Southern blot analysis to confirm gene disruption. When hybridized with probe III (*FgOs2*), no signals were detected from the genomic blot of deletion mutant strains, while the expected sizes of bands (5.3 kb *Eco*RI and 2.9 kb *Pst*I bands) were observed on the blot from the WT strain. Further evidence in support of the successful gene disruption was obtained with probe II (*hph*), showing the expected sizes of *Xho*I (3.6 kb) and *Kpn*I (7.8 kb) bands. DIG-labeled probes were prepared by using primers listed in Table S2.

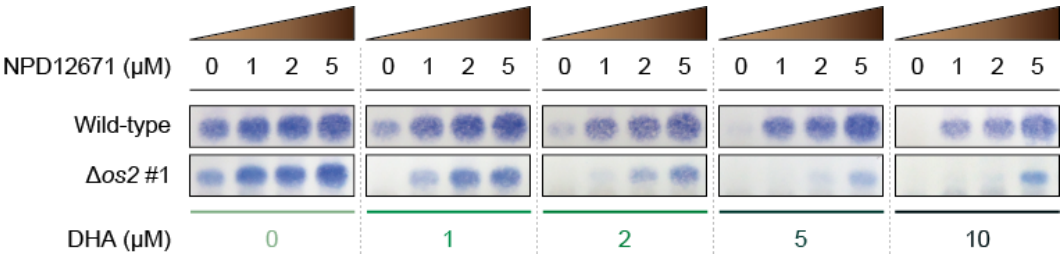

Figure S10. Competitive effect of NPD12671 and DHA on trichothecene production by the wild-type and Δ*FgOs2* mutant strains. The trichothecene assay was performed by the 24-well plate culture method. At 72 h, the 15-ADON production in the YS_60 culture was analyzed by TLC as described in Methods.

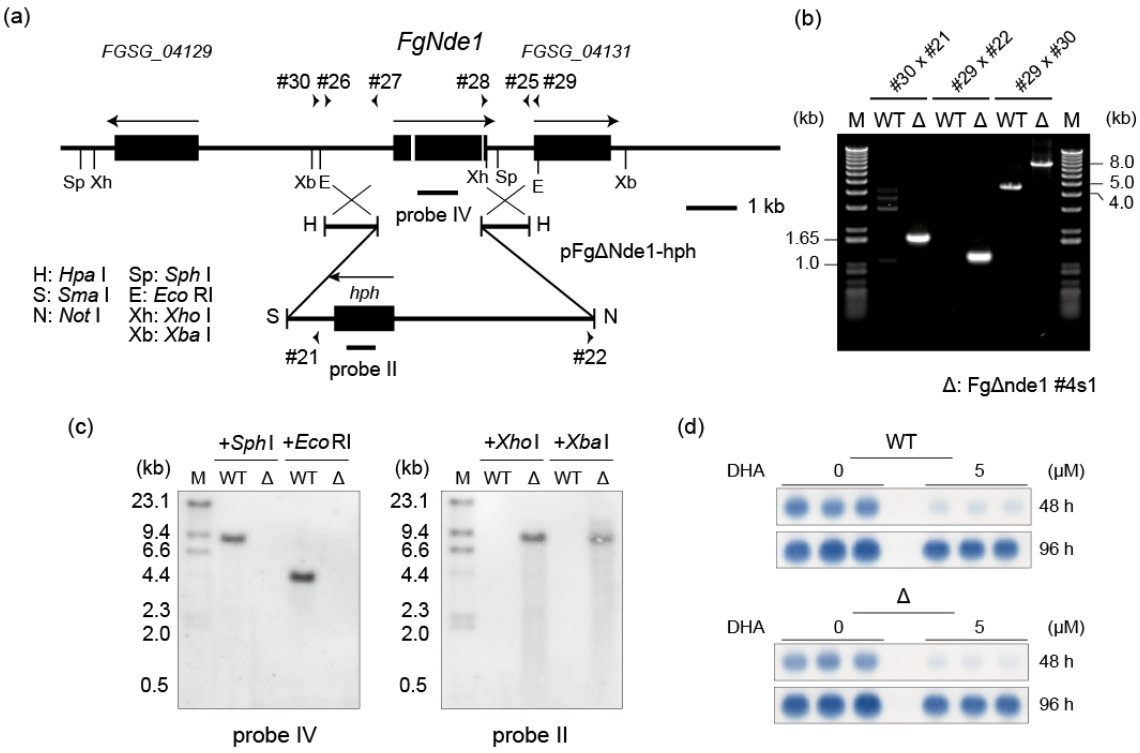

Figure S11. Disruption of *FgNde1* in *F. graminearum* JCM 9873. (a) Strategy of the *FgNde1* gene (FGSG_04130) disruption. The *FgNde1* disruption vector pFgΔNde1-hph was constructed by replacing the whole coding region of *FgNde1* with pCSN43 that contains the *hph* cassette by the inverse PCR (IPCR) method[8] (see Table S2 for primer sequences). (b) PCR confirmation of the gene disruption. PCR was performed using primers that specifically amplify the junction between the *FgNde1* gene-flanking region and gene disruption vector (#30 × #21 and #29 × #22) and primers that amplify across the deleted region (#29 × #30). Expected bands characteristic of the *FgNde1* disruption (Δ) were amplified with primers #30 and #21 (1.6 kb), #29 and #22 (1.1 kb), and #29 and #30 (7.8 kb); an expected amplicon size of 4.5 kb was obtained with primers #29 and #30 from the wild-type (WT) genome. (c) Southern blot analysis to confirm gene disruption. When hybridized with probe IV (*FgNde1*), no signals were detected from the genomic blot of mutant strain *FgΔnde1* #4s1, while the expected sizes of bands (8.2 kb *Sph*I and 4.5 kb *Eco*RI bands) were observed on the blot of the WT strain. Further

evidence in support of the successful gene disruption was obtained with probe II (*hph*), showing the expected sizes of *Xho*I (8.1 kb) and *Kpn*I (7.9 kb) bands. DIG-labeled probes were prepared by using primers listed in Table S2. (d) Trichothecene production by the WT and Δ*FgNde1* mutant strains. The trichothecene assay was performed in triplicate with the 24-well plate culture method.

References

(1) Sun, C., and Zhou, B. (2016) The molecular and cellular action properties of artemisinins: what has yeast told us? *Microb. Cell 3*, 196-205.

(2) Li, W., Mo, W., Shen, D., Sun, L., Wang, J., Lu, S., Gitschier, J. M., and Zhou, B. (2005) Yeast model uncovers dual roles of mitochondria in action of artemisinin. *PLoS Genet. 1*, e36.

(3) Sun, C., Li, J., Cao, Y., Long, G., and Zhou, B. (2015) Two distinct and competitive pathways confer the cellcidal actions of artemisinins. *Microb. Cell 2*, 14-25.

(4) Takahashi-Ando, N., Tokai, T., Yoshida, M., Fujimura, M., and Kimura, M. (2008) An easy method to identify 8-keto-15-hydroxytrichothecenes by thin-layer chromatography. *Mycotoxins 58*, 115-117.

(5) Nakajima, Y., Maeda, K., Ohsato, S., Kanamaru, K., Kobayashi, T., and Kimura, M. (2016) Nuclear localization and relative stability of the zinc finger domain of TRI6 trichothecene regulator. *JSM Mycotoxins 66*, 13-15.

(6) Tokai, T., Koshino, H., Takahashi-Ando, N., Sato, M., Fujimura, M., and Kimura, M. (2007) *Fusarium Tri4* encodes a key multifunctional cytochrome P450 monooxygenase for four consecutive oxygenation steps in trichothecene biosynthesis. *Biochem. Biophys. Res. Commun. 353*, 412-417.

(7) Maeda, K., Tanaka, A., Sugiura, R., Koshino, H., Tokai, T., Sato, M., Nakajima, Y., Tanahashi, Y., Kanamaru, K., Kobayashi, T., Nishiuchi, T., Fujimura, M., Takahashi-Ando, N., and Kimura, M. (2016) Hydroxylations of trichothecene rings in the biosynthesis of *Fusarium* trichothecenes: evolution of alternative pathways in the nivalenol chemotype. *Environ. Microbiol. 18*, 3798-3811.

(8) Banno, S., Kimura, M., Tokai, T., Kasahara, S., Higa-Nishiyama, A., Takahashi-Ando, N., Hamamoto, H., Fujimura, M., Staskawicz, B. J., and Yamaguchi, I. (2003) Cloning and characterization of genes specifically expressed during infection stages in the rice blast fungus. *FEMS Microbiol. Lett. 222*, 221-227.